NASA CR 178093

An Evaluation of Descent Strategies for TNAV-Equipped Aircraft in an Advanced Metering Environment ATOPS

Final Report

K. H. Izumi, R. W. Schwab, J. L. Groce, M. A.Coote
Boeing Commercial Airplane Company
Seattle, Washington

Prepared for
NASA TCV
Contract: NAS1-17635

National Aeronautics and
Space Administration

December 1986

NASA CR 178093

An Evaluation of Descent Strategies for TNAV-Equipped Aircraft in an Advanced Metering Environment ATOPS

Final Report

K. H. Izumi, R. W. Schwab, J. L. Groce, M. A.Coote
Boeing Commercial Airplane Company
Seattle, Washington

TABLE OF CONTENTS

LIST OF TABLES

LIST OF FIGURES

LIST OF FIGURES (Concluded)

1.0 SUMMARY

When 4D RNAV operations are used in a time-based en route metering environment, the performance of various descent strategies in mixed traffic operations and the compatibility of different descent strategies will become increasing areas of concern. An investigation was conducted of the effects on system throughput and fleet fuel of utilizing various descent strategies, both individually and in combination. The study was in support of the NASA Advanced Transport Operating Systems (ATOPS) Flow Management Avionics Research Studies program and was performed under NASA contract. The three strategies considered were clean-idle Mach/CAS, constant flightpath angle (CFPA) Mach/CAS, and fuel optimal.

The flow management evaluation model (FMEM), used in a previous NASA contract to study the effects of various levels of time navigation (TNAV) fleet equipage on air traffic control (ATC) operations and fuel efficiency, was modified for this study. The model was updated to include path definition capabilities for three Boeing airplane types, the B737-300, B747-200, and B767-200, which were assumed to represent the gamut of air carrier turbojet traffic. Traffic inputs consisted of airplane pairs that entered the simulation at a common altitude (37,000 ft), common speed (0.78 Mach), and common distance (200 nmi) from the meter fix. Three 4D RNAV absorbable (elapsed) times were used.

Results indicated that, for the assumed simulation conditions and arrival traffic distribution at a typical en route metering (ERM) airport where the 737 category of airplane comprised almost 88% of all arrivals, the optimal strategy had a fuel consumption advantage at the expense of a slight reduction in throughput over the other two strategies. However, parametric analyses indicated that the CFPA and, to a lesser extent, the clean-idle were less susceptible to throughput degradation than the optimal when airplane type mixes and strategy mixes were varied.

2.0 INTRODUCTION

The NASA Advanced Transport Operating Systems (ATOPS) Flow Management Avionics Research Studies program is identifying requirements for the use of advanced avionics capabilities in the current and projected FAA time-based en route metering system (ref 1). General and interim path definition algorithms have been designed and an interim algorithm tested in simulation and in flight.

The Federal Aviation Administration (FAA) has several advanced flow management concepts under study or development. These include the currently operational en route metering, the automated en route ATC, and integrated flow management concepts for the future. These programs and concepts are the basic elements of the National Airspace System Plan providing transition from today's controller intensive ATC system to the highly automated system of 2000 and beyond.

The definition of alternative flow management concepts, the development of scenarios for ATOPS application, and the analysis and recommendation of further testing of scenarios were accomplished under contract NAS1-14880 TRA-112. Additional work was performed under NASA Task Requirement 1-2 of contract NAS1-16300. This included the application of a fast-time simulation of the Denver Air Route Traffic Control Center (ARTCC) to study the effects of various levels of TNAV equipage on ATC operations and fuel efficiency. The equipage study assumed all aircraft employed conventional clean-idle Mach/CAS descents.

This report describes the results of an analysis of three descent strategies and their effects on throughput (number of aircraft processed per unit time) and fleet fuel. Three strategies were considered: (1) the clean drag and idle thrust descent using Mach/CAS speeds, (2) a constant flightpath angle descent with Mach/CAS speeds, and (3) the use of an optimal speed/thrust schedule to achieve ATC time control objectives. This study was defined under Task 6 of NASA contract NAS1-17635.

This report contains objectives, assumptions, and methodology employed, a description of the candidate descent strategies considered, and an analysis of the resultant traffic throughputs and fleet fuel consumed. Conclusions and recommendations are included. A mathematical description of the optimal strategy is included in Appendix A.

3.0 SYMBOLS AND ABBREVIATIONS

η_{s1}	descent strategy probability of lead airplane
η_{s2}	descent strategy probability of trail airplane
λ_m	probability of descent strategy combination {m}
ξ	analysis time interval
σ^2	throughput variance
τ	increase in time separation
ω_k	frequency of airplane combination{k}
%	percent
AAI	airplane arrival interval
ACPH	aircraft per hour
ARTCC	air route traffic control center
ATC	air traffic control
ATOPS	advanced transport operating systems
CAS	calibrated airspeed
CFPA	constant flightpath angle
Δd	horizontal separation between aircraft
DOC	direct operating cost
d_{ref}	minimum ATC horizontal separation, 5 nmi
d_1	distance of lead airplane from meter fix
d_2	distance of trail airplane from meter fix
ERM	en route metering program
FAA	Federal Aviation Administration
FCLT	freeze calculated landing time
ft	feet
F_k	maximum flow rate of airplane combination {k}
FMEM	flow management evaluation model
4D	four dimensional
Δh	vertical separation between aircraft
h_1	true altitude of lead airplane
h_2	true altitude of trail airplane
JFK	John F. Kennedy International Airport
KCAS	calibrated airspeed in knots
kn	knot
LAX	Los Angeles International Airport
NASA	National Aeronautics and Space Administration
lb	pound
min	minute
nmi	nautical miles
ORD	Chicago O'Hare International Airport
p_{cf}	frequency of CFPA strategy aircraft arrivals
p_{cl}	frequency of clean-idle strategy aircraft arrivals
p_{opt}	frequency of optimal strategy aircraft arrivals
p_{737}	frequency of B737 airplane arrivals
p_{747}	frequency of B747 airplane arrivals
p_{767}	frequency of B767 airplane arrivals
R_m	maximum flow rate for mixed strategy traffic combination {m}
RNAV	radio navigation

3.0 SYMBOLS AND ABBREVIATIONS (Concluded)

sec	second
T	system throughput
Δt_k	minimum time separation for airplane combination {k}
$(\Delta t_k)_i$	initial time separation for airplane combination {k}
TNAV	time navigation
v_{g2}	groundspeed of trail airplane

4.0 OBJECTIVES, ASSUMPTIONS, AND METHODOLOGY

The objectives of the study were to analyze and recommend a preferred descent strategy or strategies for use by 4D RNAV-equipped airplanes in future ATC operations that will have time-based metering. The strategy options evaluated for this study were clean-idle Mach/CAS descents, constant flightpath angle Mach/CAS descents, and point-mass optimal descents using variable speed and thrust schedules throughout the descent. The analysis and recommendation of one strategy over another were based on two criteria: fleet fuel usage and system throughput.

The study assumed a future ATC environment when most air carrier and other high performance aircraft will have advanced flight management systems with time navigation (TNAV) capabilities. Also assumed for this future ATC environment was an advanced air traffic control system that will have the ability to maximize the traffic throughput rate by adjusting spacings over a meter fix based on predicted relative separation requirements. This ATC advanced flow management system would be an extension of the current en route metering (ERM) system.

A composite U.S. fleet mix for the 1995 time period was assumed. This mix was based on extrapolations of current traffic trends at Denver, Dallas-Ft. Worth, and Minneapolis-St. Paul international airports. In the study, the effects of other fleet mix assumptions were also evaluated. Study results for Chicago O'Hare, John F. Kennedy, and Los Angeles international airports were also included.

The approach that was taken in this study to determine a preferred descent strategy is illustrated in Figure 1. The two steps taken for this analysis were first the performance of a separation analysis and then a throughput analysis. The separation analysis determined the minimum separation required for zero conflicts between a sequential airplane pair, flying from 200 nmi and cruise altitude to a meter fix at 10,000 ft and 250 KCAS. For each airplane in the traffic pair, inputs to the separation analysis included an assumed elapsed time, descent strategy, airplane type, and weight. Both airplanes entered the simulation at a common altitude of 37,000 ft and speed of 0.78 Mach in order to examine the influence only of descent strategy on conflicts (and therefore throughput), while controlling the effects of differences in initial altitude and speed. The pair was initially separated at cruise altitude by 5 nmi, which corresponds to a time separation of 0.67 min. Outputs of the separation analysis included zero-conflict fuel usage for each airplane and closest approach separation for the pair. For each airplane pair, a maximum flow rate value was computed. Maximum flow rate is the equivalent number of airplanes crossing the meter fix, while satisfying the zero-conflict criterion. These individual maximum flow rates for aircraft pairs were inputs to the throughput analysis.

The throughput analysis generated an expected flow rate for a particular arrival traffic distribution by airplane type. Required inputs were traffic frequencies, i.e., the probabilities of occurrence in the arrival fleet of each of the pairs. The throughput analysis combined the maximum flow rate and fuel data for each pair with the frequency data to determine a fleet fuel usage and the system throughput. The throughput analysis was performed for each of the three strategies over a parametric range of airplane type mixtures (at all three elapsed times) and over a parametric range of descent strategy mixtures for an assumed typical arrival distribution (for the short elapsed time only).

5.0 MODELING

A revised version of the flow management evaluation model (FMEM), originally developed by Boeing to conduct a NASA-funded investigation of mixed TNAV equipage traffic in an en route metering (ERM) environment (ref. 2), was used to conduct the sensitivity analysis.

5.1 FMEM ADAPTATION

The FMEM simulates arrival traffic operations at an airport participating in the ERM program. The model was specifically configured to represent the Denver Air Route Traffic Control Center (ARTCC) airspace and arrival operations at Denver Stapleton International Airport. Airplanes are assigned landing slots based on a first-come first-served mechanization and the minimum time separation interval, known as the airplane arrival interval (AAI). The resultant schedule determines required meter fix times for all arrival traffic. ERM guarantees, or "freezes," an airplane's landing time when it is within a fixed number of flying minutes from its expected meter fix arrival time. This fixed number of minutes is called the freeze calculated landing time (FCLT) parameter. A TNAV-equipped airplane is presumed to be given its meter fix time assignment when it enters the freeze region at its freeze time. The difference between the airplane's assigned meter fix time and its freeze time is its required elapsed time, which the airplane must absorb to make good its meter fix time. The assignment process is a dynamic one and can produce varying elapsed times, depending on traffic demand.

The FMEM required adaptation to conduct an evaluation of descent strategies. Two additional descent strategies (CFPA and optimal) were added and a different algorithm for computing surveillance data was included. Some tabular performance data were replaced by polynomial expressions. Finally, the capabilities of computing traffic flow rate and inputting elapsed times were new requirements.

5.1.1 Additional Descent Strategies

Constant flightpath angle (CFPA) and fuel-optimal descent algorithms, both developed by Boeing for other studies, were adapted and included as two additional descent strategies for use by TNAV-equipped airplanes. These are described in greater detail in Section 6.0.

5.1.2 Surveillance Calculations

The optimal descent logic computes energy states in relatively small, discrete altitude steps (500 ft) in descent and time intervals (10 sec) in cruise. Linear predictions within these intervals will provide more accurate position and energy states than the corresponding waypoint-referenced calculations used in the CFPA and clean-idle implementations. The assumption of linear performance characteristics between waypoints, which can be spaced considerably far apart, can lead to errors in predicting an airplane's position and energy state. It is important to minimize these errors when path profile data of two nearby aircraft are compared to determine their relative spacing for conflict detection. While both the CFPA and clean-idle profile computation processes have always used these same integration step sizes, the intermediate calculation results were never saved but used only to compute waypoint-referenced data. The FMEM was adapted and these intermediate data are now the basis for calculating present position data.

5.1.3 Polynomial Expressions for Performance Data

The optimal logic requires smooth polynomial expressions for drag polar and fuel flow. Since the optimal logic was initially developed for the B737-300 and B767-200, the performance data for these airplane types were already in polynomial form. Therefore, fuel flow and drag polar expressions were required only for the B747-200. All other performance data were not required to be in polynomial form, which include speed limit and thrust data.

5.1.4 Elapsed Time Inputs

As described above, the assignment of meter fix times in the baseline FMEM version is a dynamic process and depends on traffic demand. The current analysis required that all aircraft absorb the same elapsed time. The metering logic thus required adaptation to accommodate the assignment of fixed elapsed times.

5.1.5 Computation of Flow Rate

The implementation of the flow rate calculation is discussed in the context of the definition of flow rate in Section 7.2.

5.2 TRAFFIC MODEL

The traffic inputs consisted of three airplane types. Each type utilized two representative gross weights, which were designated as "light" and "heavy." Historical 1984 arrival traffic data at three ERM airports were consulted to create an average annual distribution by airplane type. These distributions were the bases for the weighting factors applied to the sensitivity analysis results to obtain typical throughput figures as a function of descent strategy and elapsed time.

5.2.1 Airplane Types and Weights

Assumptions were made to equate all other commercial turbojet airplane types to the B737-300, B767-200, and B747-200. The substitutions are summarized in Table 1 and were justified on the basis that older airplane types will most likely be replaced by their modern equivalents. These three types were also considered to run the gamut of aircraft weights and performance. Two weight categories ("light" and "heavy") have been assigned to each airplane type. The selection of the weight range was dictated by two considerations: (1) a realistic range of approach weights and (2) a parametric compromise between maximum weight range and maximum delay margin. The performance characteristics of the B737-300 (CFM56-3-B1 engines), B767-200 (JT9D-7R4D engines), and B747-200 (RB-211B engines) were modeled.

Each combination of airplane type and weight for either the clean-idle or CFPA descent strategy, and initial and terminal conditions, produced high-speed and low-speed (without path stretching) descent times, corresponding to speed schedules consistent with performance envelope limitations. Table 2 lists the high- and low-speed (Mach/CAS) descent times for all combinations of airplane types, two weight categories, and two descent strategies. The optimal strategy was assumed not to produce the constraining descent times because that strategy, which is not limited to a Mach/CAS speed schedule, makes greater use of its performance envelope. This assumption was confirmed by subsequent optimal strategy runs. No airplane

was allowed to path stretch or fly faster than its high-speed descent time. Thus, certain airplane type and weight combinations defined the fastest of all low-speed times and the slowest of all high-speed descent times. These comprised the short and long elapsed times, which were imposed on all airplane types and weight categories. These times necessarily meant that certain airplane types did not use their full-time envelopes.

A higher B737 heavy weight would have produced a slower standard high-speed time. Similarly, a higher B747 heavy weight would have defined a faster standard low-speed time. Table 2 shows that the standard high-speed descent time of 1658 sec is determined by the heavy B737 (CFPA descent), and the low-speed time of 1819 sec by the heavy B747 (CFPA).

5.2.2 Arrival Traffic Distribution

The three airports that are currently involved in the ERM program are Denver Stapleton International, Dallas-Fort Worth International, and Minneapolis-St. Paul International. 1984 annual arrival statistics were obtained (ref. 3) for these three airports.

The U.S. domestic and international arrival distributions among the three types are shown in Table 3. The table indicates that the proportion of the B737 type is essentially the same at these three airports, while the mixes between the B767 and B747 vary. In addition, the B737 represents a substantial percentage (about 90%) of the total arrival traffic. Table 3 also summarizes air carrier turbojet arrival operations at all domestic U.S. airports and indicates that the ERM typical distribution is very similar to the U.S. average. The ERM average type mix was used to illustrate system throughput performance at a typical airport.

6.0 DESCENT STRATEGY CHARACTERISTICS

The term descent strategy, as utilized in this study, referred to the definition of the algorithms and procedures for predicting the arrival flightpath (limited to the vertical flightpath in this study) of an airplane from the entry point at cruise altitude to the meter fix at 10,000 ft. The descent strategy determined the manner in which accelerations/decelerations were performed, the speeds flown in cruise and descent, and the use of thrust and drag. The descent strategy was constrained to traverse a fixed distance from entry point to meter fix during a fixed time period. The three descent strategies compared in this study were clean-idle, CFPA, and optimal.

6.1 CLEAN-IDLE DESCENT

The clean-idle strategy was based on descending at idle thrust with flaps, speed brakes, and gear retracted. The fixed elapsed time from entry point to meter fix was achieved using a modified binary search technique iteratively to determine the required speeds. A one-dimensional search was obtained by defining the cruise Mach to be equal to the descent Mach. Furthermore, the descent speed was defined in terms of a Mach/CAS family of speeds, where for every Mach there exists only one value of CAS. This was accomplished by partitioning the descent speed envelope using a critical altitude model. This model mathematically described the variation of critical altitude (the altitude where a constant Mach descent transitioned to a constant CAS descent) with true airspeed. Thus, for each value of Mach selected by the search algorithm, a cruise Mach and descent Mach/CAS were fully defined.

For each iteration of descent Mach, the clean-idle strategy computed an acceleration or deceleration at cruise altitude, a cruise segment, a descent segment, and another acceleration or deceleration segment at meter fix altitude. The cruise distance was adjusted so that the total distance for all segments equals the required distance from entry point to meter fix. Accelerations or decelerations were performed at maximum climb thrust or idle thrust, while in level flight in a clean configuration. A cruise segment was then computed at the descent Mach.

Descent computations were based on point-mass, steady-state equations of motion that were solved for small altitude steps during descent. Rate of descent was computed as a function of thrust (set to idle thrust) and drag utilizing a high-speed drag polar formulation combined with lift as a function of weight. The descent was integrated over the entire altitude range by summing time, distance, and fuel values at each altitude step.

Figure 2 plots altitude and distance versus time for simulations of B737 and B747 clean-idle descents. The entry point altitude is 37,000 ft and is 200 nmi from the meter fix at 10,000 ft. The elapsed time from entry point to meter fix is 1658 sec (27.6 min). A common time reference is used for both airplanes and shows that the B737 is initially 5 nmi (0.67 min at Mach 0.78) ahead of the B747. Differing cruise/descent Machs for the two airplanes result in the B747 gradually reducing separation from the B737 to zero. At 14.5 min, the B747 reaches top of descent, while the B737 continues cruise until 17.6 min. The B737 remains above the B747 until 24.7 min where it crosses below the B747, at which point it has increased separation back to 5 nmi ahead of the B737.

6.2 CFPA DESCENT

This strategy was based on descent at a constant inertial flightpath angle. Since winds were neglected in this study, the descent was also at a constant airmass flightpath angle. The algorithms and procedures were identical to those of the clean-idle strategy described in Section 6.1, except that the descent segment itself was computed differently.

Descent calculations were based on point-mass, steady-state equations of motion solved for small altitude steps during descent. The rate of descent at each altitude step was defined geometrically from the descent speed and the flightpath angle (which was a fixed value). The thrust required was then computed as a function of rate of descent and drag. Drag was first computed based on a high-speed drag polar that assumed speed brakes were retracted. If the resulting thrust was less than the minimum available (idle thrust), then the drag was recomputed based on extending speed brakes such that the required flightpath angle was maintained using idle thrust. Time, distance, and fuel values were summed over the descent as in the clean-idle strategy.

Figure 3 plots altitude and distance versus time for simulations of B737 and B747 CFPA descents. All conditions except descent strategy are identical to those of Figure 2. The B747 is shown to reduce separation gradually from the B737 to zero. Top of descent is reached at 14 min for both airplanes. Differing speed schedules cause the B747 to fall behind and above the B737 during descent.

6.3 OPTIMAL DESCENT

This strategy utilized Pontryagin's Minimum Principle to assert that a fuel-optimal airplane trajectory for a fixed terminal time was actually an optimal direct operating cost (DOC) trajectory for a certain cost of time.

Algorithms for the optimal strategy were based on solving the general system of differential equations of motion commonly employed for aircraft trajectory computations in the longitudinal plane. Since the equations were fifth-order and nonlinear, a tenth-order, two-point boundary value problem resulted from application of Pontryagin's Minimum Principle. Singular perturbation theory was utilized to simplify the solution by separating the system dynamics into slow and fast modes to reduce a high-order problem to a series of lower order problems. The resulting formulation separated the solution into the inner region (descent) and the outer region (cruise). Since the inner region still required solution of two-point boundary value problems, the energy state approximation was utilized to reduce this to only one state equation. A Fibonacci search parameter optimization scheme was then utilized to generate speed and thrust commands, which minimized DOC. DOC was defined in terms of time and fuel costs, which were combined to yield the cost index, defined as time cost divided by fuel cost. A Newton-Raphson search technique was then employed to find the cost index providing the required elapsed time. The resulting thrust, speed, and fuel parameters were optimal values. Further details of the mathematical formulation of this optimization are contained in Appendix A.

Figure 4 plots altitude and distance versus time simulations of B737 and B747 optimal descents. All conditions except descent strategy are identical to those of Figures 2 and 3. The B747 is shown to reduce separation gradually from the B737 to zero at 7 min, and to begin descent at 10.5 min. The B737 begins descent at 16 min as the B747 moves ahead of the B737. The B747 then slows, and the B737 moves ahead at 23.3 min and drops below the B747 at 24.5 min.

7.0 TRAFFIC FLOW RATE ANALYSIS

This section addresses the question of what arrival flow rate can be sustained by each of the descent strategies under consideration. Assumptions were made that all aircraft were constrained to the same initial cruise altitude and speed, that the same 4D elapsed time requirements were imposed on all traffic, and that an advanced ATC system adjusted spacings at the entry point to ensure conflict-free operations throughout all descents. A separation analysis was conducted to determine minimum time separation data for all pairs of aircraft type and weight. Then, system throughput for each strategy and elapsed time was computed from the minimum time separation data and an assumed arrival traffic distribution. Additional throughput studies were made for three major U.S. airports that represented other arrival traffic distributions. Finally, the effect on system throughput of mixing descent strategies was examined.

7.1 SEPARATION ANALYSIS

Since the intent of the analysis was to determine minimum time separation (referenced at the simulation's entry point) to support a minimum ATC distance separation throughout the descent, the computation of the loss in flow rate was done as part of a conflict detection analysis. That is, when a loss of minimum separation occurred, a determination was made of the corresponding loss in flow rate. An ATC separation violation was said to occur when two proximate airplanes were simultaneously within 5 nmi horizontally and 2000 ft (above FL290) or 1000 ft (at or below FL290) vertically of each other. The result of the separation analysis was a set of minimum time separations at the entry point for a given elapsed time and descent strategy.

7.1.1 Simulation Assumptions

Traffic inputs were pairs of aircraft, consisting of any two combinations of airplane type and weight category. Therefore, for each descent strategy and elapsed time, 36 runs were made. In addition to constraining each airplane to a fixed initial altitude and speed, each pair was initially separated by 5 nmi. This corresponded to an initial time separation of 0.67 min at 37,000 ft and 0.78 Mach. Both aircraft also ended their descents at the meter fix at an altitude of 10,000 ft and speed of 250 kn (CAS). Since the aircraft arrival interval (AAI) was also set at this initial time separation and every airplane had to absorb the same elapsed time for a specific run, the pair was also separated by 0.67 min by the time the trail airplane reached the meter fix. Because of the differences in speed between the aircraft pair throughout the descent, time separation varied considerably. The analysis time interval ξ was defined as the interval between the freeze time of the first airplane and the meter fix arrival time of the second airplane.

7.1.2 Separation Data

Horizontal and vertical separation are defined as

$$\Delta d = d_2 - d_1$$
$$\Delta h = h_2 - h_1$$

where 1 and 2 refer to the lead and trail aircraft, respectively, d_i is the distance (in nmi) of the ith airplane from the meter fix, and h_i is the true altitude (in feet) of the ith airplane. These

data were computed at every simulation clock step throughout the analysis time interval ξ. Separation histories (Δd versus Δh) for the example pair of aircraft discussed in Section 6 are plotted in Figures 5 through 7. Each plot presents separation histories for all three strategies and for a particular elapsed time, starting at an initial horizontal separation of 5 nmi ($\Delta d = 5$) and vertical separation of 0 feet ($\Delta h = 0$) and ending at a nominal $\Delta d = 3.23$ and $\Delta h = 0$. Each curve represents the progression of relative separation. Successive points on a curve are separated by a simulation time interval of 30 sec.

In the figures, for both the optimal and clean-idle strategies, the B747 is shown to overtake the B737 ($\Delta d < 0$) at cruise altitude. Figure 5 is the descent speed profile plot for the short elapsed time case. In all three strategies, it is seen that initially the B737 decelerates at cruise altitude in order to meet its required elapsed time. Conversely, the B747 accelerates at cruise altitude. In the cases of the clean-idle and CFPA strategies, these characteristics are a result of the Mach/CAS speed schedules dictated by the respective descent strategy implementations. The behavior in the optimal strategy case arises when the two airplane types change to their respective speeds at cruise altitude to minimize fuel. The magnitudes of the changes for both airplane types are greater for the optimal strategy than those for the other two and explain the greater horizontal separation (at $\Delta h = 0$) excursions for the optimal in Figure 5. For the long elapsed time, the optimal aircraft exhibit the same characteristics, while in the CFPA and clean-idle cases, the B747 decelerates instead.

The B747 begins its descent before the B737 ($\Delta h < 0$). The B737 eventually gains on the B747 in altitude until it goes lower in altitude briefly before both aircraft reach the meter fix. In the CFPA case, the B737 loses its horizontal lead position to the B747 but descends first ($\Delta h > 0$), as Figure 5 shows.

The magnitudes of the horizontal displacement in the regions where ATC separation criteria have been violated are indications of the relative increase in time separation required of the trail airplane at the entry point to preclude conflicts.

If the B747 were the lead aircraft, the separation histories are almost the reverse of the situation above. For all three strategies, the B747 accelerates as soon as it begins its delay absorption ($\Delta d > 5$) and begins its descent first. This is exemplified in Figure 8, which corresponds to a required elapsed time of 1819 sec. This figure also illustrates the fact that the final horizontal separation among all three strategies is not necessarily 3.23 nmi, because each profile computation of a particular airplane type and weight is accurate to within ± 1 sec of the required elapsed time.

Examination of speed profile data of the heavy B737 and heavy B747 for the short elapsed time, for example, indicates the differences in true air speed throughout the descent. These are illustrated in Figures 9 through 11. For all strategies, the B737 immediately decelerates while the B747 accelerates after their respective freeze times (elapsed time = 0). The final cruise speeds for the clean-idle and CFPA cases are determined by the speed transition (Mach/CAS) model, while the cruise speed for the optimal strategy is selected primarily for best fuel consumption.

7.1.3 Minimum Time Separations

The expression for required time separation is given by

$$\Delta t_k = (\Delta t_k)_i + \tau \quad (1)$$

where Δt_k = minimum time separation between airplane pair {k}
$\Delta(t_k)_i$ = initial time separation between airplane pair {k}
τ = increase in time separation between airplane pair {k}

In these series of runs, $(\Delta t_k)_i$ = 0.67 min. The increase in time separation is the increment of time beyond the initial time separation by which the trail airplane is required to lag the lead airplane to ensure conflict-free operations. Therefore, τ is correlated to a loss of horizontal separation when a conflict develops. If d_{ref} is the minimum ATC horizontal separation criterion, Δd is the horizontal separation at an arbitrary time t, and v_{g2} is the groundspeed (in knots) of the trail aircraft at time t, τ (in minutes) is then given by

$$\tau = 60\ (d_{ref} - \Delta d)/v_{g2}$$

Because of the 5-mile rule,

$$\tau = (300 - 60\Delta d)/v_{g2} \quad (2)$$

It is seen from Equation (1) that the minimum Δt_k to prevent conflicts throughout the analysis time interval ξ occurs when τ is maximum within ξ. This minimum Δt_k is referred to in this analysis as the minimum time separation. The program computes Δt_k whenever separation minima are violated and compares its value with a previously stored maximum value. If required, the new maximum will replace the previous value. This procedure is carried out until the trail airplane crosses the meter fix. Within the limitations that these calculations are made at 30-sec intervals, a value close to the true minimum time separation will have been computed.

These values of minimum time separation will be used to determine maximum flow rates in Section 7.2.

Table 4 contains the resultant minimum time separation data.

7.2 FLOW RATE ANALYSIS

As discussed above, this concept of flow rate was based on having assured that ATC separation criteria were not violated. Flow rate is therefore related to minimum time separation, as defined in Paragraph 7.1.3.

7.2.1 Flow Rate

If minimum time separation Δt_k (in minutes) is the conflict-free time separation between a pair of aircraft, defined as pair k, on the same route, then its flow rate (in aircraft per hour, ACPH) is

$$F_k = 60/\Delta t_k \quad (3)$$

If the loss of time separation τ between a particular pair of aircraft does not reach its maximum until the trail airplane reaches the meter fix, then Δd in Equation (2) is determined by the time separation between the aircraft and the groundspeed of the trail airplane at the meter fix.

Maximum flow rates equivalent to the minimum time separation data of Table 4 are presented in Table 5.

Because of the implementation of the 4D logic in the FMEM, path solutions were accurate to within ±1 sec. Thus, if the lead airplane were 1 sec early and the trail airplane 1 sec late, the greatest time spacing at the meter fix was 0.70 min (0.67 min + 2 sec), with a final spacing of 3.38 nmi. Because the groundspeed of the trail airplane was 288.85 kn (250 kn CAS at 10,000 ft altitude), the limiting (worst case) flow rate could have been as high as 59.69 ACPH, based on calculations using Equations (1) and (3). The conclusion is that all flow rate values, assuming no other perturbations, cannot exceed a rate of 59.69. This value served as a check on the validity of the results of Table 5. If the profile calculation had no time error, then the nominal limiting throughput was 57.77 ACPH. Note that, for the pair of airplanes consisting of the same type and weight, flow rate values were 57.77 in most cases. This is because the path solutions were exactly the same for both airplanes, the path solutions incurred the same error, and therefore the relative time spacing was the nominal airplane arrival interval, or 0.67 min. The limiting flow rate calculation was based on multiple traffic on a common arrival route. Nevertheless, for the same reasons mentioned, the flow rate for any pair of aircraft, even when arriving on different routes converging at the meter fix, is still limited to 59.69 ACPH.

Adjusted flow rate, or the degradation of flow rate, as a function of time is plotted for each elapsed time in Figures 12 through 14. The final flow rate value at the end of ξ is referred to as the maximum flow rate for a given aircraft pair, strategy, and elapsed time. All three strategies are presented on the same plot for comparison. The cases are the same as discussed in Section 6 and Paragraph 7.1.2. The initial flow rate at the entry point is always 89.55 because the initial time separation is 0.67 min. Elapsed time is referenced to the first airplane's freeze time, or the beginning of ξ. These figures show that loss of minimum separation occurs immediately. Flow rate degrades steadily for all three strategies until somewhere in the middle of descent. The conflict-free, maximum flow rates are achieved between 10 and 17 min, depending on strategy.

7.2.2 Parametric Traffic Analysis

System throughput is here defined as the expected flow rate. This definition presumes a traffic distribution and large sample populations. Statistical analyses can be conducted in which the frequencies of airplane types are used.

Weighted averages and standard deviations can be computed. If weighting factors or arrival probabilities of pairs of aircraft are given by ω_k (if k represents a pair of particular aircraft type and weight mix), then throughput, T, is given by

$$T = \sum_{k=1}^{M} \omega_k F_k \tag{4}$$

where M is the number of combinatory pairs of airplane type and weight, or 36, and F_k is given by Equation (3). Its variance is computed by

$$\sigma^2 = \sum_{k=1}^{M} \omega_k (F_k - T)^2 \tag{5}$$

For each descent strategy and elapsed time combination, families of throughput curves were generated from Equation (4) as functions of a particular airplane type percentage with a second type as a parameter. Varying airplane type mixes subject to

$$p_{737} + p_{747} + p_{767} = 1$$

produces throughput sensitivity relationships, where p_{737}, p_{747}, and p_{767} are the arrival probabilities of the B737, B747, and B767, respectively. Figures 15 through 17 show the effect of varying B737 proportions with the B767 proportion as parameter cross-plotted with those with the B747 as parameter, for all three elapsed times and a clean-idle strategy. Corresponding plots for the CFPA and optimal strategies are presented in Figures 18 through 20 and Figures 21 through 23, respectively. The clean-idle, CFPA and, to a lesser extent, the optimal results show that, for fixed B747 levels, throughputs are relatively constant for all ranges of B737 and B767 mixes. However, for increasing levels of the B747, throughput favors a higher percentage of the B767 than that of the B737.

For the optimal strategy at fixed B747 levels, throughput performance depends more on the ratio between the B737 and B767 than do the clean-idle and CFPA strategies. For both the short and medium elapsed times and fixed levels of the B747 from 0% to 50%, minimum throughputs are generated when the B737 constitutes 50% of all arrivals. For the long elapsed time, 40% B737s are required for minimum throughputs for 0% to 50% fixed B747 levels. This implies that for the optimal strategy, system throughputs for 50% B737 levels will be minimum regardless of the relative mixes between the B747 and B767. However, these reductions in throughput are not as significant as when the percentage of B747s is increased from zero to some intermediate level, for either fixed levels of the B737 or the B767.

Figures 15 through 23 also demonstrate that increasing the levels of the B747 has more of a deleterious effect on throughput for the optimal strategy than for the CFPA strategy. Table 6 summarizes the deterioration of throughput under two scenarios. The first considers what happens when, with the traffic always maintained at equal B737 and B767 levels, the numbers of B747s is increased from 0% to 40% of all arrivals; and the second, when the percentage of B747s is increased from 0% to 50% when no B767s are part of the traffic.

For all strategies, increasing the 4D times generally decreases throughput for the same traffic mix. This effect is less pronounced for the CFPA strategy than for either the clean-idle or optimal strategy. For example, with no B767s and when the B737 and B747 are equally distributed, throughput degrades by 3.58%, 1.54%, and 2.72% for the clean-idle, CFPA, and optimal strategies, respectively, when the 4D time is increased from 1658 to 1819 sec. Similarly, when the B737/B747 ratio is 30/70, throughput reductions are 4.14%, 2.22% and 6.02%.

While the best possible throughputs are the same regardless of strategy, the worst throughputs are achieved by the optimal strategy. Table 7 summarizes the best achievable results and the conditions under which they occur. The worst throughputs are shown in Table 8. In the worst possible scenario, when all aircraft engage the optimal strategy and there are no B767s, increasing the percentage of the B747 from 0% to 70% of all arrivals (and therefore reducing the B737 percentage from 100% to 30%) would reduce system throughput by 15.1%.

7.2.3 Typical Arrival Traffic Analysis

The typical traffic distribution (par. 5.2.1) is influenced by the predominance of the B737 type. Weighting factors for the typical traffic distribution are shown in Table 9.

Weighted throughput means and standard deviations derived from Equations (4) and (5) are given in Table 10. Weighted means for fuel are also provided.

As shown in Table 3, the B737/B737 combinations contribute 77.2% (19.3% x 4) of all aircraft pairs in typical arrival traffic. The average of the individual flow rates for the B737, extracted from Table 5, in their four weight combinations, and the average minimum time separations related to these flow rates, are summarized in Table 11. Based on the fact that the B737's optimum cruise altitude and speed are essentially 37,000 ft and 0.78 Mach, respectively, these results indicate that, for almost 80% of all traffic combinations, throughputs will be the same, regardless of descent strategy and required elapsed time. Furthermore, an entry point arrival interval of almost 1.04 min is sufficient to generate a throughput of approximately 58 ACPH, with no ATC intervention. A separation analysis of the B737 pairs shows that maximum flow rate is insensitive to descent strategy because an initial separation of almost 1.04 min (dictated by the constraints at the meter fix) is of such a magnitude that variations in separation behavior among the three strategies are not significant.

7.2.4 Analyses of Other Distributions

While the previous section examined a typical airport, some major U.S. airports experience somewhat different mixes of arrivals. The cases of John F. Kennedy (JFK) International, Los Angeles International (LAX), and Chicago O'Hare (ORD) were considered to analyze throughput performance as a function of different arrival traffic distributions. The summary of 1984 distributions by airplane type in Table 3 shows the B737 aircraft type only constitutes 42.6% of all arrivals at JFK because of offloading of short-haul operations to nearby municipal airports. LAX and ORD show increasing frequencies of the B737.

Weighted throughputs as functions of elapsed time for the typical ERM airport and three others are plotted in Figure 24. From the trends demonstrated in Figure 24, it is apparent that system throughput decreases as a single airplane type becomes less dominant in the total traffic mix. Furthermore, the optimal descent strategy is susceptible to greater throughput degradation than either of the other two strategies as traffic becomes more equally distributed among the three airplane types.

7.2.5 Mixed Strategy Analysis

Since it is probable that airlines will choose different flight management system implementations of descent strategy, the effect on throughput of mixing descent strategies was examined. For a given elapsed time, system throughput is the weighted average of all aircraft, weight and descent strategy combinations:

$$T = \sum_{m} \lambda_m R_m \qquad (6)$$

where combination m refers to an aircraft pair of specific type, weight, and strategy combinations and R_m is the maximum flow rate associated with m. The expression consists of 324 terms since either of the pair can assume one of 18 airplane type-weight-strategy conditions. The frequency λ_m is also related to the weighting factor ω_k of Equation (4):

$$\lambda_m = \omega_k \eta_{s1} \eta_{s2}$$

where ω_k is the arrival probability of an aircraft pair of type-weight combinations k, η_{s1} is the descent strategy probability of aircraft 1 and η_{s2} is the strategy probability of aircraft 2.

A parametric study, for only the short elapsed time case, was also performed. In a fashion similar to the development in Paragraph 7.2.4, families of throughput curves were generated from Equation (6), which are functions of a particular descent strategy with a second strategy as a parameter, subject to:

$$p_{opt} + p_{ci} + p_{cf} = 1$$

where p_{opt}, p_{ci}, and p_{cf} are the arrival probabilities of optimal-, clean-idle-, and CFPA-strategy aircraft, respectively. The throughput sensitivity relationships are plotted in Figure 25, with the optimal strategy as the independent variable. These curves correspond to the assumed typical traffic distribution and the short elapsed time. The trends expressed in the figure indicate that the optimal strategy has a greater influence on throughput than any of the other strategies. In particular, increasing the percentage of aircraft (for the assumed distribution) employing optimal descents degrades system throughput faster than corresponding increases of either the CFPA or clean-idle-equipped aircraft. On the other hand, an increase in CFPA aircraft as a percentage of total traffic improves throughput for either a fixed level of clean-idle or optimal aircraft. When none of the aircraft uses clean-idle, changing the fleet from 0% CFPA to full CFPA equipage increases throughput by 2.7%, whereas for traffic containing no CFPA aircraft, throughput improves by 2.6% when the traffic mix changes from 0% clean-idle to 100%. Generally, for a fixed level of optimal aircraft, throughput is insensitive to variations in CFPA/clean-idle mixes, as Figure 25 shows, but slightly favors the CFPA as the optimal percentage increases.

Figure 26 shows the results of a similar analysis performed for JFK International where the arrival traffic consists mostly of B737 and B747 aircraft in equal numbers. System throughput is shown to be insensitive to mixes between the clean-idle and CFPA strategies for a fixed level of optimal. Throughput appears to be a function primarily of the level of optimal-equipped aircraft.

7.3 FUEL ANALYSIS

In this analysis, the notion of maximum flow rate for an airplane pair assumed that the fuel used by the pair was independent of their relative spacing for a specific descent strategy and elapsed time. The requirement that no conflicts occur was satisfied by the model's determining a sufficient minimum initial spacing rather than by issuing an ATC clearance. Therefore, the model computed for each airplane type the minimum achievable fuel consumption for a given descent strategy and elapsed time combination. If the minimum time separation (par. 7.1.3) between an airplane pair were reduced to increase system throughput, techniques would have to be employed to avert conflicts (speed reduction, nominal path offset, etc.). If any airplane were still required to make the same elapsed time, the loss in time related to path changes must be made up elsewhere in descent by a speed increase or, if possible, path shortening. These perturbations produce fuel penalties, which are not quantified here. As long as the system was able to support the required time separations without traffic demand exceeding throughput capacity, these zero-conflict fuel usage results could be considered applicable.

Delay time was absorbed in each of the strategies by using a descent speed schedule which was unique for each elapsed time/strategy combination. The cruise portion of the descent accounted for 50% to 65% of the 200-nmi distance flown and was the major contributor to fuel usage. Comparisons of fuel usage were made for three values of delay times, 1658, 1739, and 1819 sec.

7.3.1 Airplane Comparison

Fuel burn values are shown in Table 12 for each airplane type, elapsed time, and strategy. The overall trend is for fuel usage to decline as elapsed time is increased, which is a result of the airplane being able to cruise at a lower, more fuel-efficient speed.

A comparison of the differences in fuel usage can be seen in Table 13. Clean-idle is used as the baseline for each airplane and elapsed time. The optimal descent strategy reduced descent fuel burn by approximately 0% to 4%, while the CFPA strategy produced a penalty of as much as 6%.

7.3.2 Fleet Comparison

A combined weighted fuel burn has been derived to represent the typical mix of airplanes arriving at a typical ERM airport. The data, as in previous developments, were derived from the 1984 Airport Activity Statistics and used Dallas/Ft. Worth, Denver, and Minneapolis arrival statistics.

The fuel usage data are shown in Figure 27 for each strategy as a function of elapsed time. The data show that when the system throughput is under the limiting throughput value, the optimal strategy has the potential for a fuel advantage over the clean-idle strategy of approximately 1.5%, compared with a 2.6% penalty for the CFPA strategy. Fuel usage comparisons are also made for Chicago O'Hare, Los Angeles, and John F. Kennedy international airports (figs. 28 through 30) and demonstrate similar trends as for the typical airport.

8.0 CONCLUSIONS AND RECOMMENDATIONS

The annual system throughput data in Table 10 assumed three descent strategies, three levels of absorbable (elapsed) times, specific initial traffic conditions, and a typical arrival aircraft type traffic distribution, in which the B737 comprises 88% of all arrivals. The CFPA descent strategy enjoys a slight throughput advantage over the clean-idle and optimal strategies. The differences among the strategies, however, are small for all elapsed times. This phenomenon results from the large numbers of the B737 airplane type in the arrival traffic as a whole. System throughputs, in fact, are close to the limiting throughput of 57.77 ACPH, as derived in Paragraph 7.2.1. The implications are that the limit will only be achieved if all traffic consisted of the same airplane type and weight combination, and that traffic composed of a more equitable distribution of airplane types would only decrease the expected throughput. If the traffic distribution were to show a smaller contribution by the B737 type and correspondingly larger influence of the other two types, system throughput rates for all strategies would deteriorate, with the optimal strategy incurring the greatest loss and the CFPA the least. These trends are demonstrated by the results of the Los Angeles, Chicago O'Hare, and John F. Kennedy international airports' studies and the throughput sensitivity relationships in Figures 15 through 23. However, in the near- and far-term traffic environment, the actual arrival mix is forecast to remain similar to the typical distribution assumed for the analysis.

Fleet-fuel savings results corresponding to conflict-free operations show the reverse trend. While the optimal strategy had the lowest throughput, it also used the least fuel. If the optimal strategy is used as the reference, fuel burn penalties of the clean-idle and CFPA strategies are 37.7 and 104.7 lb for the short; 17.1 and 58.7 lb for the medium; and 27.4 and 57.6 lb for the long elapsed times, respectively.

Therefore, the assumptions and conditions employed in this analysis favor the optimal strategy for fuel usage, with a slight disadvantage in throughput relative to the other two strategies for the assumed traffic distribution. However, if the individual maximum flow rate figures of Table 5 bear some relationship to, or are in some way measures of, the extent to which ATC must intervene in order to increase throughput, then a greater fuel penalty will be experienced by those airplane combinations having lower maximum flow rates. Actual fuel penalties due to reduced flow rate cannot be established until conflicts can be dynamically resolved in the simulation. However, an approach is presented in Appendix B to quantify the fuel usage and conflict workload sensitivities to various arrival rates under the same distance and conflict-free assumptions made earlier.

The preceding analysis assumes restricted airspace capacity because of the single (common) route and zero-conflict criteria. No excess delay absorption techniques or conflict resolution were considered within the system. Airspace capacity can be increased if traffic can be distributed over several paths. These distributed configurations include parallel paths on the same route, additional routes, or combinations of merging routes. These formulations enable the input (entry point) flow rates to match or exceed the output (meter fix) flow rate. However, because of separation requirements at the meter fix, its airspace feeder system throughput would still be constrained to the nominal limiting throughput value. Since system throughput with a typical ERM arrival traffic distribution is close to the limit, it would appear that an effort to analyze the effects of increasing airspace capacity would not justify the slight possible gains in throughput. As long as one airplane type dominates the arrival statistics, system

performance may be largely insensitive to descent strategy. When system throughput is expected to be near the limit, the study results suggest that no ATC or airline benefits will be achieved by increasing airspace capacity or decreasing the minimum, zero-conflict spacing required between aircraft.

Implicit in this zero-conflict, single-route analysis is the assumption that the initial spacing between consecutive aircraft be made as large as required to satisfy the zero-conflict criterion. In the present analysis, that spacing was only a little more than 1 min on the average, or an in-trail spacing of 7.74 nmi. This also suggests that descent strategy is not an issue when the demand on the system is low.

To summarize, the comparative findings of the current analysis are as follows:

1. For a typical arrival distribution, the optimal strategy is the most fuel efficient with a slight throughput disadvantage.
2. The CFPA strategy generates the greatest throughput for zero conflicts, regardless of arrival traffic distribution, while the optimal generates the least.
3. The optimal strategy consumes the least fuel per aircraft for zero conflicts, regardless of arrival traffic distribution, while the CFPA consumes the most.
4. In mixed strategy traffic, throughput is the most sensitive to the percentage of optimal-strategy airplanes.
5. The clean-idle and CFPA strategies can be mixed interchangeably with negligible throughput differences.

Two additional analyses are suggested for further investigation of descent strategies for use in a metered environment. One study assumes arrival traffic in which the three airplane types enter the metering system at their optimum altitudes and speeds. The second examines the effect of changing the metering freeze radius (freeze calculated landing time, FCLT) on throughput performance.

Whether the current results can be extrapolated to throughput performance of traffic in which airplane types enter the metering system at their optimum speeds and altitudes is not apparent. It appears that the combinations of slower airplanes entering the system ahead of faster ones would produce improved maximum flow rates in this configuration, because the initial conflicts at cruise altitude noted in the current analysis would probably be eliminated. This kind of analysis also lends itself to a statistical evaluation like the one in Section 7, as opposed to requiring a Monte Carlo simulation. Initial separations can also be defined in this context that will result in zero conflicts. Similar parametric analyses can be carried out to study throughput sensitivities to mixed traffic and mixed strategies.

The effect of varying the FCLT parameter also would be a significant study since the relative proportions of descent and cruise segments will alter maximum flow rate performance.

9.0 REFERENCES

1. *Local Flow Management/Profile Descent Avionics Research System Requirements and Benefit Analysis,* J. T. Burghart and E. A. Delanty, The Boeing Commercial Airplane Company, May 1978, NASA CR-145341.

2. *An Investigation of TNAV-Equipped Aircraft in a Simulated En Route Metering Environment,* J. L. Groce, R. W. Schwab, K. H. Izumi, J. A. Taylor, and C. H. Markham, The Boeing Commercial Airplane Company, NASA CR-178031, May 1986.

3. *Airport Activity Statistics of Certificated Route Air Carriers,* Office of Management Systems (Federal Aviation Administration) and Office of Aviation Information Management (Research and Special Programs Administration), December 1984.

APPENDIX A. THE OPTIMAL DESCENT STRATEGY FORMULATION*

Aircraft Equations of Motion

The aircraft model used for the optimal strategy formulation assumed a point mass approximation, that is, state variables describing the vehicle attitude were either omitted or used as control variables. The energy-state approximation of the point-mass longitudinal model of the aircraft, in the presence of wind, was taken to be in conventional state variables as follows:

$$\frac{dx}{dt} = (V + V_w) \tag{A.1}$$

$$\frac{dm}{dt} = -f \tag{A.2}$$

$$\epsilon \frac{dE}{dt} = \frac{(V + V_w)(T - D)}{mg} - V_w \gamma \tag{A.3}$$

where x was the range, V the airspeed, V_w the windspeed, m the mass, f the fuel flow rate, E the energy height, γ the flightpath angle, T the thrust, and D the drag. The second term on the right hand side of Equation (A.3) is normally small and can usually be neglected. ϵ is a small "singular perturbation" parameter that arises as a consequence of the particular aircraft dynamics and an appropriate choice of scaling the equations of motion. The energy height E was related to the altitude and the groundspeed through

$$E = h + (V + V_w)^2/2g \tag{A.4}$$

The airspeed V and the thrust T are the control variables, varying within the limits:

$$T_{min} \leq T \leq T_{max} \tag{A.5}$$

$$V_{min} \leq V \leq V_{max} \tag{A.6}$$

Both V_{min} and V_{max} were functions of altitude and represented the controllability and structural and performance limitations on the aircraft. The airplane model also involved the fuel flow rate f(h, M, T), the drag polar $C_D(C_L,M)$, which is modeled using multiple regression methods, and minimum and maximum thrusts $T_{min}(M, h)$, $T_{max}(M, h)$. M denotes the Mach number, C_D the drag coefficient, and C_L the lift coefficient.

Performance Index

The optimization problem was to steer the system, Equations (A.1) through (A.3), from an initial state (x_i, m_i, E_i) at t_i to a final state (x_f, m_f, E_f) at fixed final time t_f so that the fuel spent is minimized. Equivalently, the expression

$$J = \int_{t_i}^{t_f} C_f f \, dt \tag{A.7}$$

was minimized where C_f was the cost of fuel.

*Adapted from *Four-Dimensional Fuel-Optimal Guidance in the Presence of Winds,* A. Chakravarty, Journal of Guidance, Control, and Dynamics, Vol. 8, No. 1, January-February 1985

Pontryagin's Minimum Principle

The Hamiltonian for Equations (A.1) through (A.3) and (A.7) was

$$H_1 = C_f f + \lambda_x(V + V_w) - \lambda_m f + \lambda_E \frac{(V + V_w)(T - D)}{mg} \tag{A.8}$$

where λ_x, λ_m, and λ_E were the range, mass, and energy adjoint variables respectively. Pontryagin's minimum principle states that the Hamiltonian is minimum along an optimal trajectory. Furthermore, since the final time is fixed, and H_1 is not an explicit function of time, H_1 is constant along the optimal trajectory and given by

$$\min_{T,V} \{H_1\} = K \tag{A.9}$$

K has the units of cost per unit time, and if $C_t = -K$ is selected, Equation (A.9) may be rewritten

$$\min_{T,V} \left[C_t + (C_f - \lambda_m)f + \lambda_x(V + V_w) + \lambda_E \frac{(V + V_w)(T - D)}{mg} \right] = 0 \tag{A.10}$$

along the optimal trajectory. It therefore reduces to a direct operating cost (DOC) optimization problem with free terminal time and cost parameters C_f and C_t. The balance between fuel and time costs was expressed by the so-called cost index

$$CI = \frac{C_t}{C_f} \tag{A.11}$$

The traditional units used in the cost index are C_t in dollars per hour and C_f in cents per pound. The 4D optimization problem was now reduced to finding the correct C_t or CI, for assigned arrival time t_f. If the nominal trajectory corresponded to maximum range cruise (MRC), for which $C_t = 0$, a fuel-optimal trajectory for any delay would correspond to a negative cost of time, contrary to usual DOC choices.

Cruise Cost Function

As $\epsilon \rightarrow 0$, the outer solution (according to singular perturbation theory) was reduced to

$$\min_{\substack{h,V \\ (T=D)}} \left[C_t + (C_f - \lambda_m)f + \lambda_x(V + V_w) \right] = 0 \tag{A.12}$$

Using Pontryagin's minimum principle, we further get

$$-\lambda_x = \min_{h,V} \left[\frac{C_t + (C_f - \lambda_m)f}{(V + V_w)} \right]_{T=D} \tag{A.13}$$

where the ratio to be minimized is the cruise cost function.

Climb/Descent Cost Function

During climb/descent, the independent variable was defined as $\tau = t/\epsilon$ for climb and $\sigma = (t - t_f)/\epsilon$ for descent such that as $\epsilon \rightarrow 0$, τ, and σ were finite over climb and descent, respectively. Equation (A.10) was therefore transformed into

$$\min_{T,V} \left[C_t + (C_f - \lambda_{mc})f + \lambda_{xc}(V + V_w) + \lambda_E \frac{(V + V_w)(T - D)}{mg} \right] = 0 \qquad (A.14)$$

where λ_{mc} and λ_{xc} corresponded to the values during cruise. To minimize Equation (A.14), the energy adjoint

$$\lambda_E = - \begin{matrix} \min \\ V,\ D<T\leq T_{max} \\ \max \\ V,\ T_{min}\leq T<D \end{matrix} \left[\frac{C_t + (C_f - \lambda_{mc})f + \lambda_{xc}(V + V_w)}{(T - D)(V + V_w)/mg} \right] E \qquad (A.15)$$

The minimization was done to get the climb solution, and the maximization to get the descent solution. The ratio in Equation (A.15), to be optimized at current energy E, was called the climb/descent cost function.

APPENDIX B. DESCENT STRATEGY PERFORMANCE SENSITIVITY TO ARRIVAL RATE

The main body of the report described an analysis whose results were based on separation of en route 4D arrival traffic to maximize throughput, without requiring ATC conflict intervention. Throughput and fuel usage performance did not assume accumulation of en route or terminal area delays, but instead depended on the existence of an advanced metering system that could space arrivals at the entry point to satisfy the zero-conflict criterion.

On the other hand, if the rate of arrival traffic were increased, delays required to maintain minimum separation could accumulate to an extent that fuel usage figures for traffic conditions (airplane type mix and descent strategy) demonstrating lesser zero-conflict throughput performance will produce worse overall fuel economy. The analysis below attempts to quantify throughput, average fuel usage, and conflict workload for a range of input arrival rates for equally-spaced traffic.

The basic assumption is that, if Δt_i is the minimum time separation between airplane pair i (interarrival time required to maintain nonconflicting separation between pair i; see par. 7.1.3), the trail airplane will require delay of magnitude $(\Delta t_i - T)$ when input traffic time separation, T, is closer than Δt_i. That is, at some point, input arrival rate, AR = 1/T, exceeds the ability of the system to sustain that rate at the meter fix. Another assumption is that excess delay will be taken by the trail airplane by flying a vector at its original cruise altitude and speed, beginning immediately after receiving its 4D clearance.

If input traffic of arbitrary sequence of airplane types consists of n airplane pairs, then total delay, D_n, can be written as

$$D_n = d_1(T) + [d_1(T) + d_2(T) + \cdots + d_1(T) + \cdots + d_n(T)] \qquad (B.1)$$

where D_n = total delay for n airplane pairs
T = arrival spacing between airplane pairs

$$d_i(T) = \begin{cases} 0 & \text{when } \Delta t_i \le T \\ \Delta t_i - T & \text{when } \Delta t_i > T \end{cases} \qquad (B.2)$$

Note that term $(\Delta t_i - T)$ is the delay that the trail airplane of pair i must take when initial spacing (input interarrival time) is insufficient to maintain minimum time separation needed to relieve conflict between the pair, and that for any given delay required of pair i, the same delay has to be taken by all subsequent pairs through pair n to satisfy the same conflict-free criterion. This cascading phenomenon penalizes aircraft appearing later in the traffic list.

Total fuel usage for n airplane pairs, F_n, is given by the expression

$$F_n = FB_1 + \{FB_2 + ff_2 d_1(T)\} + \cdots + \{FB_{n+1} + ff_{n+1}[d_1(T) + \cdots + d_n(T)]\} \qquad (B.3)$$

where FB_k = conflict-free fuel used by the kth airplane in meeting its 4D time
ff_k = fuel flow of kth airplane at cruise altitude and speed

and $d_i(T)$ is given by (B.2).

Total fuel is shown to depend on total accumulated delays of all n airplane pairs.

Finally, average fuel usage (per airplane) is given by:

$$\bar{F}_n = \frac{F_n}{n+1} \tag{B.4}$$

For n airplane pairs average meter fix throughput, $\bar{R}$, is given by

$$\bar{R} = \frac{n}{t_{el}} \tag{B.5}$$

where t_{el} = elapsed time between the meter fix crossings of the first and last airplanes in the traffic.

In turn,

$$t_{el} = g_1(T) + g_2(T) + \cdots + g_n(T) \tag{B.6}$$

where

$$g_i(T) = \begin{cases} T & \text{when } \Delta t_i \leq T \\ \Delta t_i & \text{when } \Delta t_i > T \end{cases} \tag{B.7}$$

Expression (B.5), evaluated with (B.6) and (B.7), implies that average throughput is 1/T when the arrival rate is small enough that no excess delay is caused by any airplane pair. Also, throughput can no longer match arrival rate when delays are needed to avoid conflicts. In particular, t_{el} decreases hyperbolically with increasing arrival rate until the first applicable airplane pair comes into conflict. For sufficiently large arrival rate, throughput no longer depends on arrival rate, but only on minimum time separations. Therefore, while throughput reaches saturation (remains constant), system delay increases according to (B.1).

Note that throughput expression (B.5) is an alternative definition to that represented by Equation (4) in Paragraph (7.2.2).

A measure of controller workload is the number of clearances that have to be issued to maintain minimum traffic separation. This is simply the number of trail airplanes among n pairs that require delay (vector) for a given arrival rate. Conflict count, N_{con}, is therefore:

$$N_{con} = c_1(T) + c_2(T) + \cdots + c_n(T) \tag{B.8}$$

where

$$c_i(T) = \begin{cases} 0 & \text{when } \Delta t_i \leq T \\ 1 & \text{when } \Delta t_i > T \end{cases}$$

The form of expressions like (B.1), (B.3), (B.6), and (B.8) implies sensitivity to the sequence of airplane types in the traffic for a fixed arrival rate. They also depend on the number of airplanes in the traffic list, that is, on the number n.

Significant performance characteristics of throughput, fuel usage, and conflict workload can be approximated if simplifying assumptions are made. Specifically, if traffic were imagined to consist of a single airplane type whose performance characteristics of minimum time

separation, Δt, and fuel flow, $\underline{ff}$, are "representative" (weightings) of the traffic mix at a given airport, then

$$\Delta t_1 = \Delta t_2 = \cdots = \Delta t_n = \Delta t$$

$$ff_1 = ff_2 = \cdots = ff_n = ff$$

The term Δt is the inverse of system throughput, such as those in Table 10 for a typical ERM airport. The term $\underline{ff}$ can be considered a weighted (according to the assumed traffic mix) fuel flow of the three airplane types used for this study. Expressions (B.4), (B.5), and (B.8) reduce to:

Approximate Fuel Usage

$$\bar{F}_n = \begin{cases} \overline{FB} & when\ \Delta t \le T \\ \overline{FB} + \frac{1}{2} n\,(\Delta t - T)\,ff & when\ \Delta t > T \end{cases} \qquad (B.9)$$

where

$$T = \frac{1}{AR}$$

and

$$\overline{FB} = \frac{1}{n+1} \sum_{i=1}^{n+1} FB_i$$

which is an expression for average undelayed fuel usage (for known strategy and 4D time), some example values of which are plotted for large $\underline{n}$ in Figures 27 through 30 in the report.

Approximate Meter Fix Throughput

$$\bar{R} = \begin{cases} \frac{1}{T} = AR & when\ \Delta t \le T \\ \frac{1}{\Delta t} & when\ \Delta t > T \end{cases} \qquad (B.10)$$

Approximate Conflict Count

$$N_{con} = \begin{cases} 0 & when\ \Delta t \le T \\ n + 1 & when\ \Delta t > T \end{cases} \qquad (B.11)$$

The following relative conclusions can be drawn from expressions (B.9) through (B.11), based on the observation that

$$(\Delta t)_{opt} > (\Delta t)_{clean} > (\Delta t)_{CFPA} \qquad (B.12)$$

Equation (B.9) indicates that at sufficiently large arrival rates fuel usage performance of the three descent strategies changes in relation to each other because the optimal strategy has lower throughput (causes the airspace to reach saturation faster) than either the clean-idle or CFPA strategy. Stated in another way, zero-conflict throughput rates as defined in this report

can be viewed as measures of susceptibility to conflicts and therefore the need to resolve them by taking additional delays (using more fuel). Although the optimal strategy requires less fuel to fly than clean-idle or CFPA when arrival rate is low, that benefit is soon lost as conflicts begin to occur because the optimal strategy creates conflicts at lower arrival rates than the others (eq. (B.11)).

Equation (B.10) shows that among the three strategies the optimal causes meter fix throughput saturation at the lowest arrival rate.

Breakpoints occur when input arrival rate equals system throughput for each strategy, which can be derived by equating the two parts of either expression (B.9) or (B.10) to each other.

A Monte Carlo simulation was also conducted to determine throughput, fuel usage, and conflict workload performance averaged over 1000 runs, using all three descent strategies at both the ERM and JFK international airports. Medium elapsed time (1739 sec) results of maximum flow rates and zero-conflict fuel usage numbers were used. Each of the 1000 runs per airport and strategy consisted of 120 airplane pairs whose sequence was randomly determined, but whose airplane type composition was constrained to mixtures enumerated in Table 3. Note that, for other values of $\underline{n}$, results would be dependent on (but not proportional to) the number of airplane pairs analyzed.

Means of fuel usage, meter fix throughput, and conflict workload are plotted in Figures B.1 through B.6 and are evaluations of expressions (B.4), (B.5), and (B.8), respectively. Maximum values of the standard deviation to mean ratio are shown in Table B.1.

These results demonstrate sensitivity to the distribution of minimum time separations $\{\Delta t_i\}$. The fuel and conflict figures illustrate two major phenomena: the effects of worst-case time separation behavior between the B737 type followed by the B747 type and the minimum attainable zero-conflict time separation. Table 5 in the main body of the report indicates at what arrival rates each strategy will experience separation violations among its pairings. B737/B747 combinations interact around 30 ACPH for the optimal strategy and around 40 ACPH for clean-idle and CFPA. The effect of greater numbers of the B747 type is evident when JFK plots are compared to ERM plots at these arrival rates. In addition, the greater sensitivity of the optimal strategy to B767/B747 and B737/B767 pairs is also manifested for arrival rates around the high-30s through the mid-40s.

The limiting flow rate in the mid-50s characterizes the minimum time separation of most airplane pairs and is graphically depicted in the conflict and fuel plots by the sharp rise in this region and by saturation in the throughput plots.

Fuel and throughput performance relative to the CFPA strategy is plotted in Figures (B.7) through (B.10). Clean-idle tracks CFPA performance closely, staying within 2.5% of CFPA's fuel requirements and within about 1% of throughput. While requiring less fuel for arrival rates not exceeding 30 ACPH, the optimal strategy uses up to 14% (ERM distribution) and 44% (JFK distribution) more fuel than the CFPA for greater arrival rates. Likewise, the optimal strategy's throughput performance degrades by up to 5% (ERM) and 13% (JFK) for arrival rates in excess of 30 ACPH.

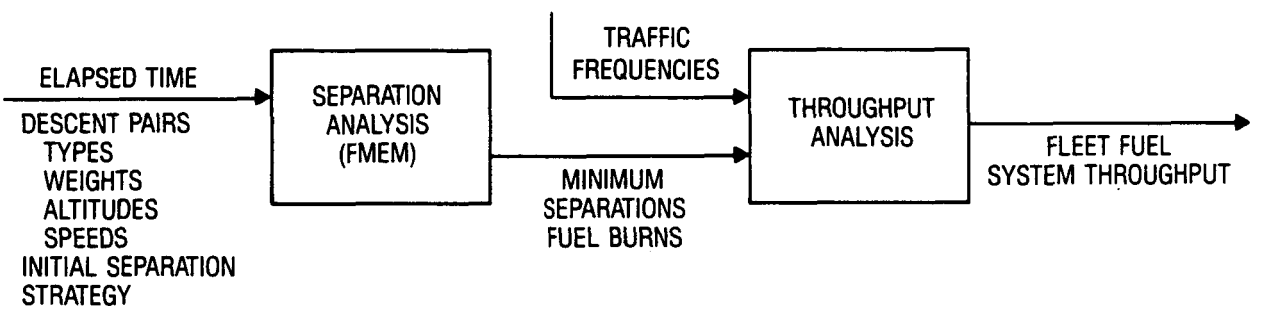

Figure 1. Descent Strategy Analysis Study Approach

Table 1. Airplane Equivalents

AIRPLANE TYPE	BOEING EQUIVALENT
DC-9 B727 B737 BAC-111 BAC-146	B737-300
B707 DC-8 A-300 A-310 B757 B767	B767-200
DC-10 L-1011 B747	B747-200

Table 2. Elapsed Time Envelopes

AIRPLANE TYPE	WEIGHT (lb x 1000)	DESCENT STRATEGY	MINIMUM ELAPSED TIME (sec)	MAXIMUM ELAPSED TIME (sec)
B737	90	Clean-Idle	1609	1883
B737	100	Clean-Idle	1648	1887
B737	90	CFPA	1617	1900
B737	100	CFPA	1658	1900
B747	475	Clean-Idle	1452	2042
B747	564	Clean-Idle	1477	1831
B747	475	CFPA	1455	2029
B747	564	CFPA	1482	1819
B767	215	Clean-Idle	1524	1972
B767	270	Clean-Idle	1529	2004
B767	215	CFPA	1523	1955
B767	270	CFPA	1527	1982

Table 3. 1984 Arrival Traffic Distributions (Percent)

(AIRPORT)	B737-300 TYPE	B767-200 TYPE	B747-200 TYPE
John F. Kennedy	42.6	11.5	45.8
Los Angeles	67.9	6.2	25.9
Chicago O'Hare	80.0	7.9	12.1
Atlanta	82.4	11.0	6.6
Denver Stapleton	86.2	7.8	6.0
Dallas/Ft. Worth	88.2	4.1	7.7
Minneapolis/St. Paul	90.6	0.8	8.6
Typical ERM Airport	87.9	4.8	7.3
U.S. Average	88.9	4.6	6.5

Data derived from *Airport Activity Statistics of Certificated Route Air Carriers,* Office of Management Systems (Federal Aviation Administration) and Office of Aviation Information Management (Research and Special Programs Administration), December 1984.

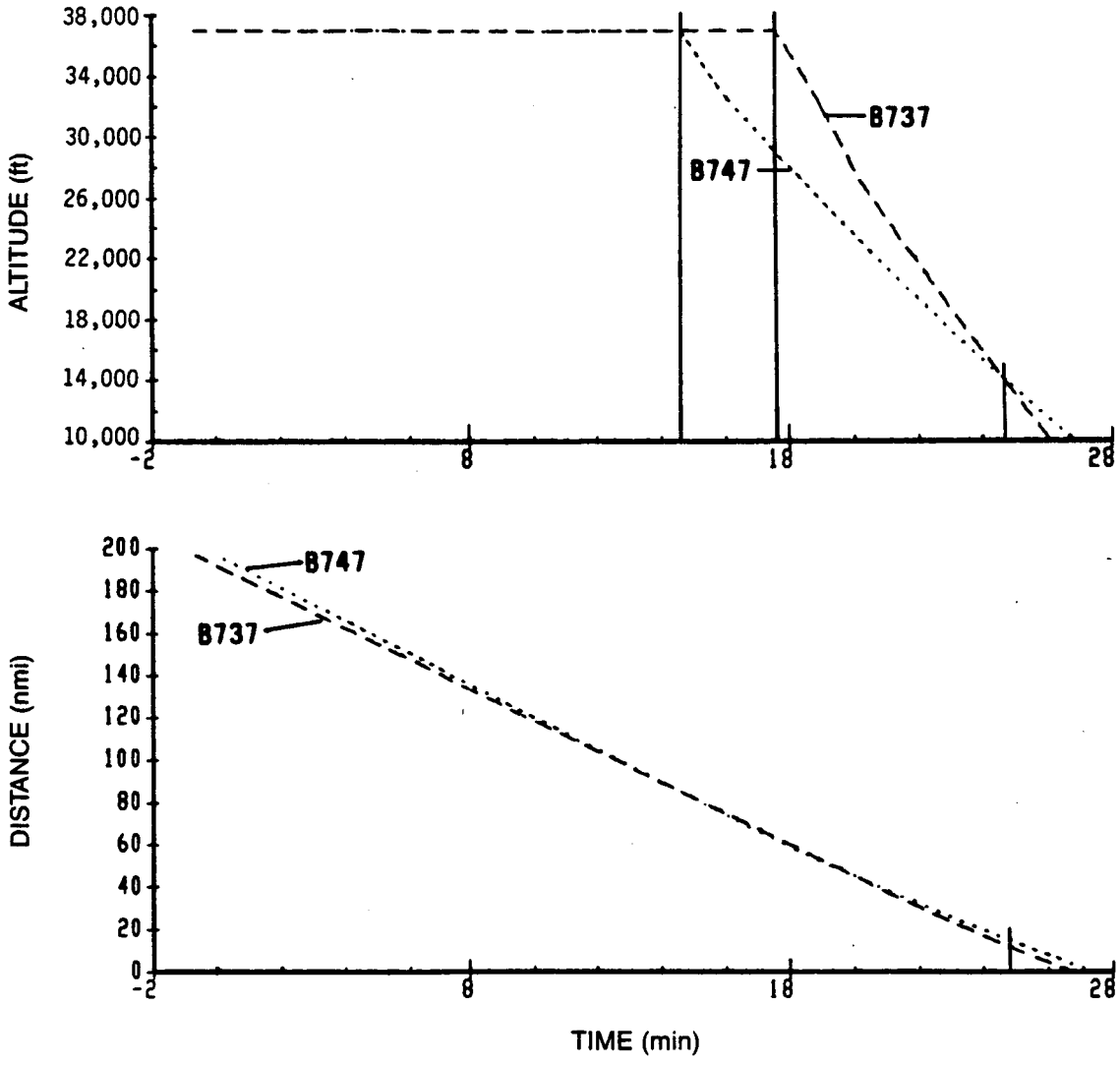

Figure 2. Clean-Idle Descent Profiles, Elapsed Time = 1658 sec

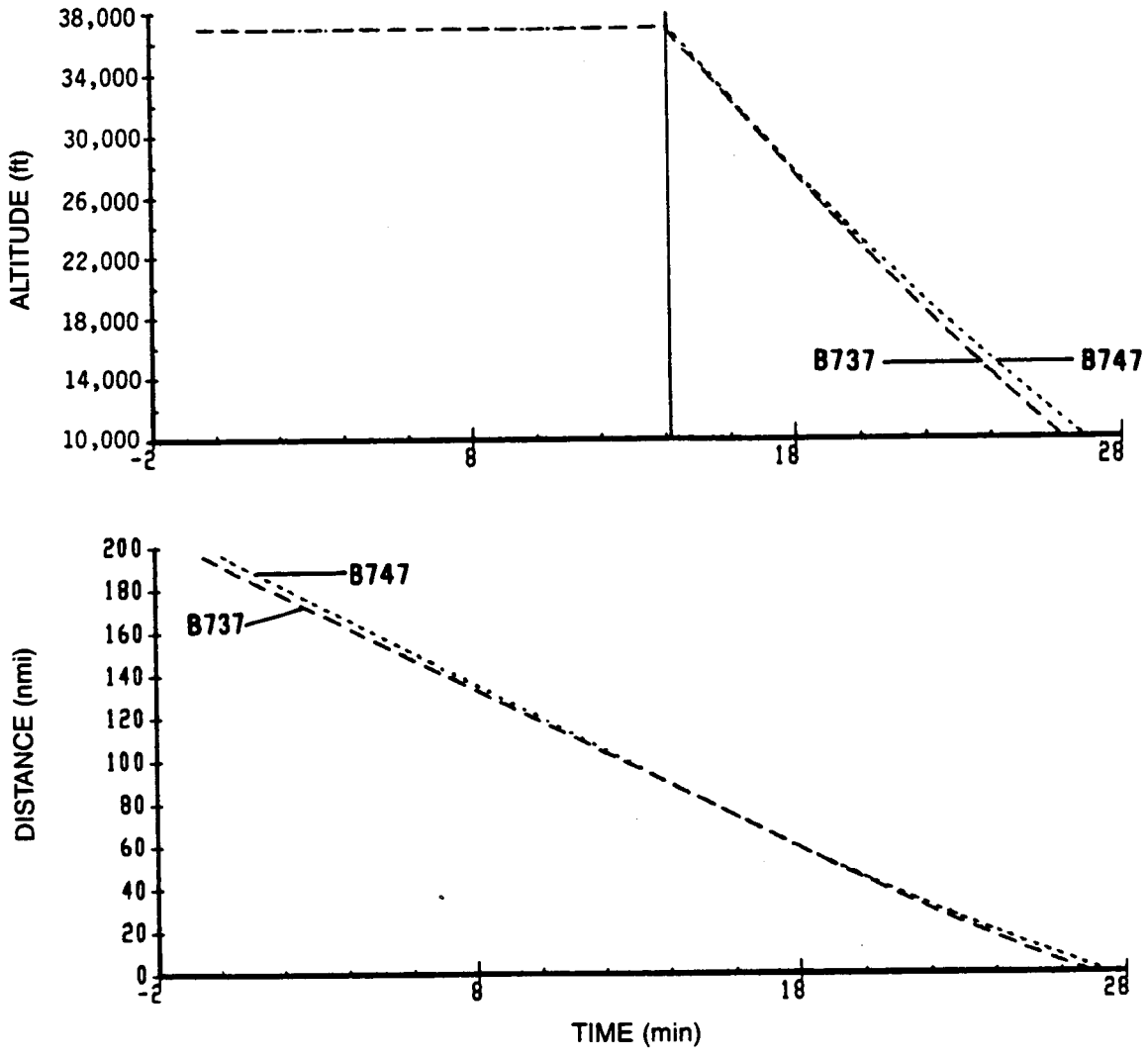

Figure 3. CFPA Descent Profiles, Elapsed Time = 1658 sec

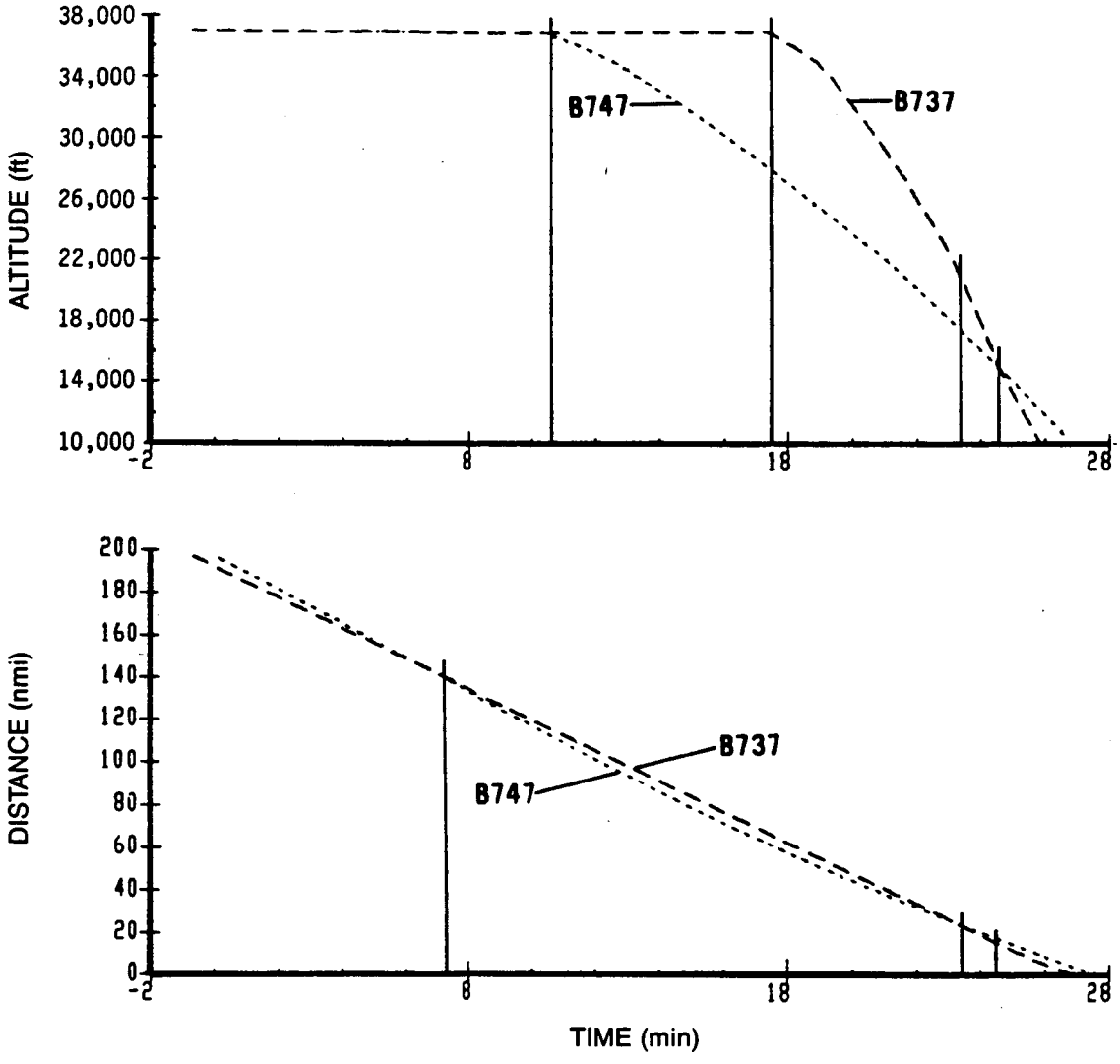

Figure 4. Optimal Descent Profiles, Elapsed Time = 1658 sec

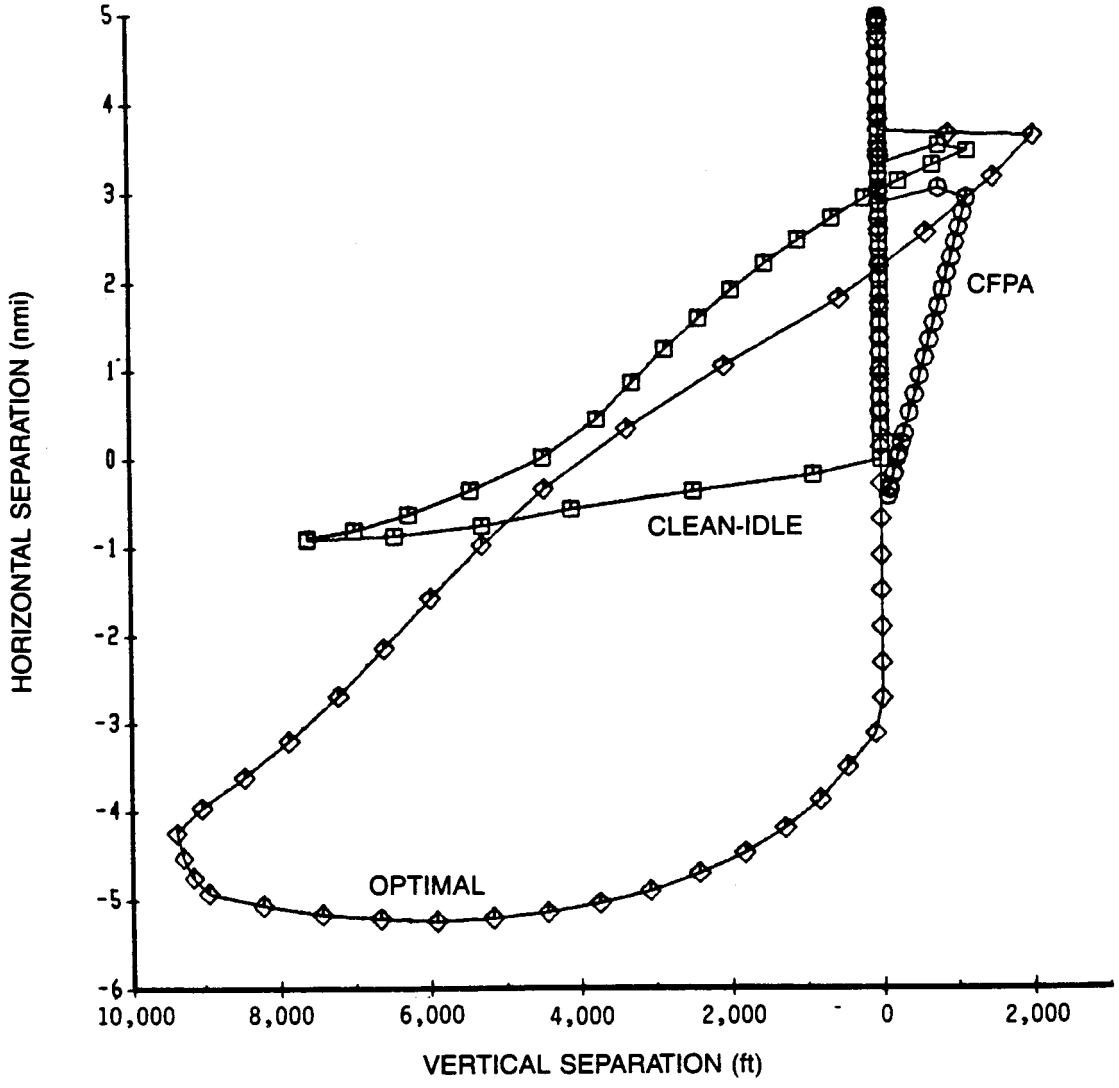

Figure 5. Comparative Separation Data—Heavy B737 Followed by Heavy B747, Elapsed Time = 1658 sec

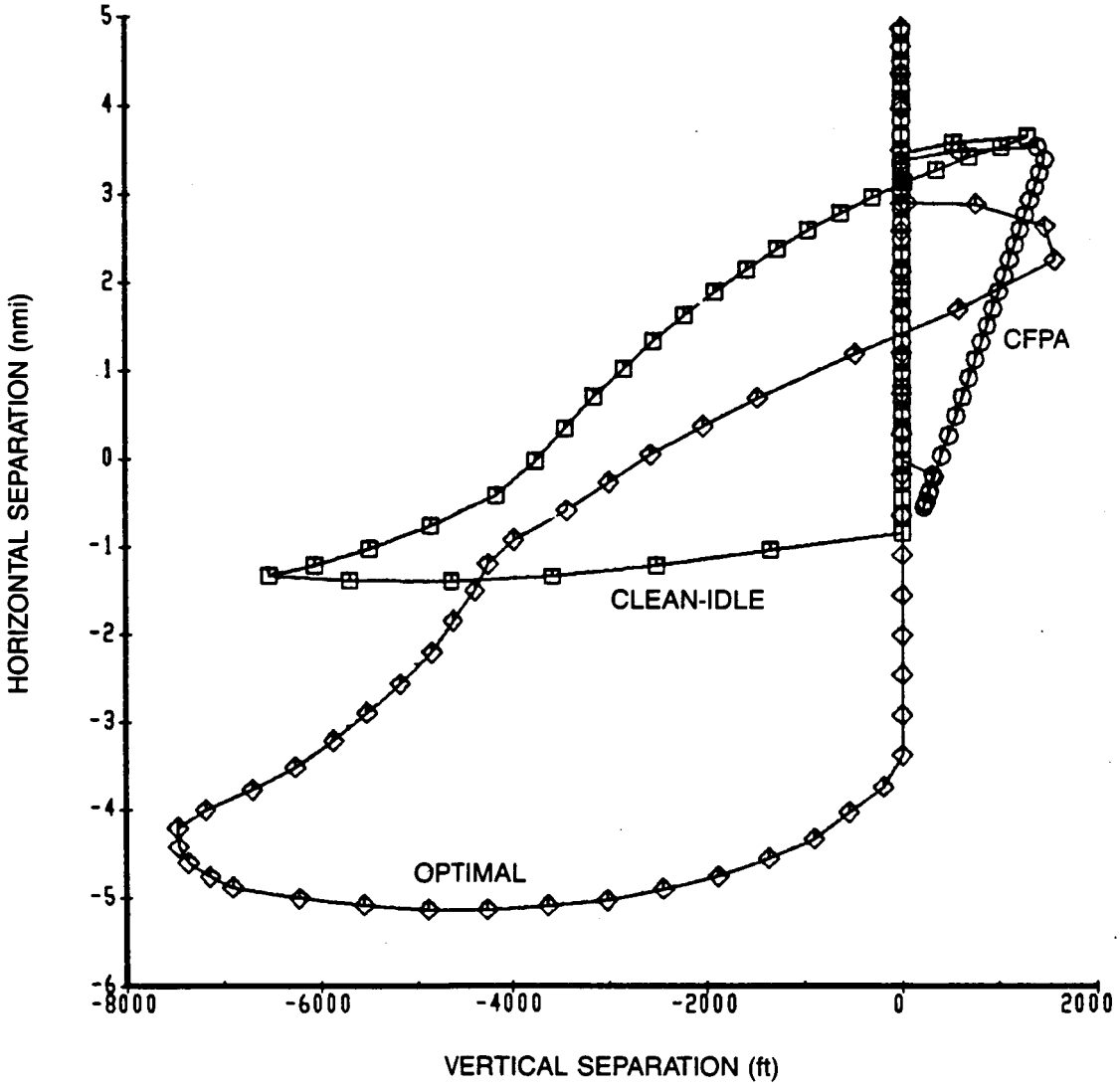

Figure 6. Comparative Separation Data—Heavy B737 Followed by Heavy B747, Elapsed Time = 1739 sec

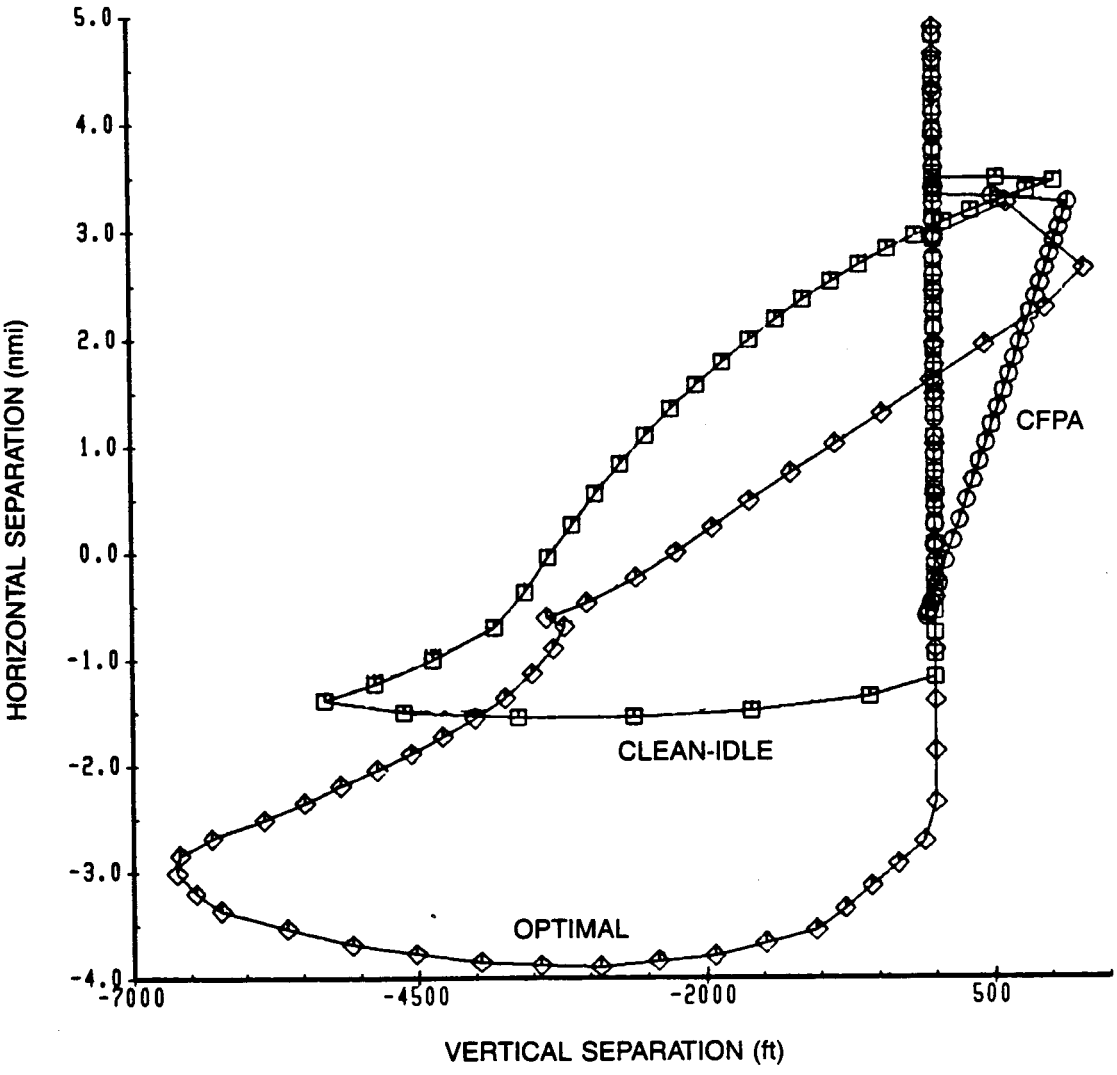

Figure 7. Comparative Separation Data—Heavy B737 Followed by Heavy B747, Elapsed Time = 1819 sec

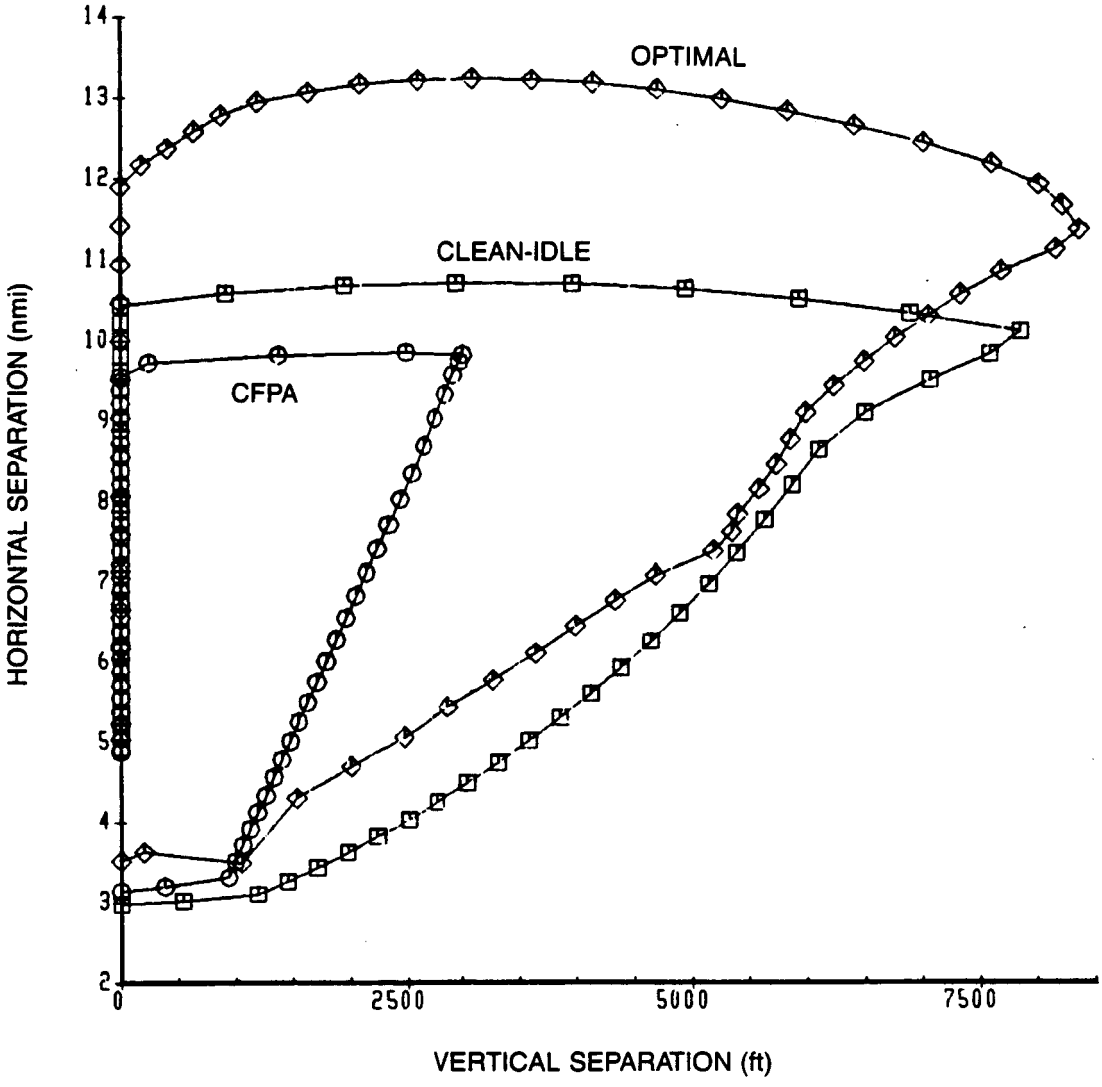

Figure 8. Comparative Separation Data—Heavy B747 Followed by Heavy B737, Elapsed Time = 1819 sec

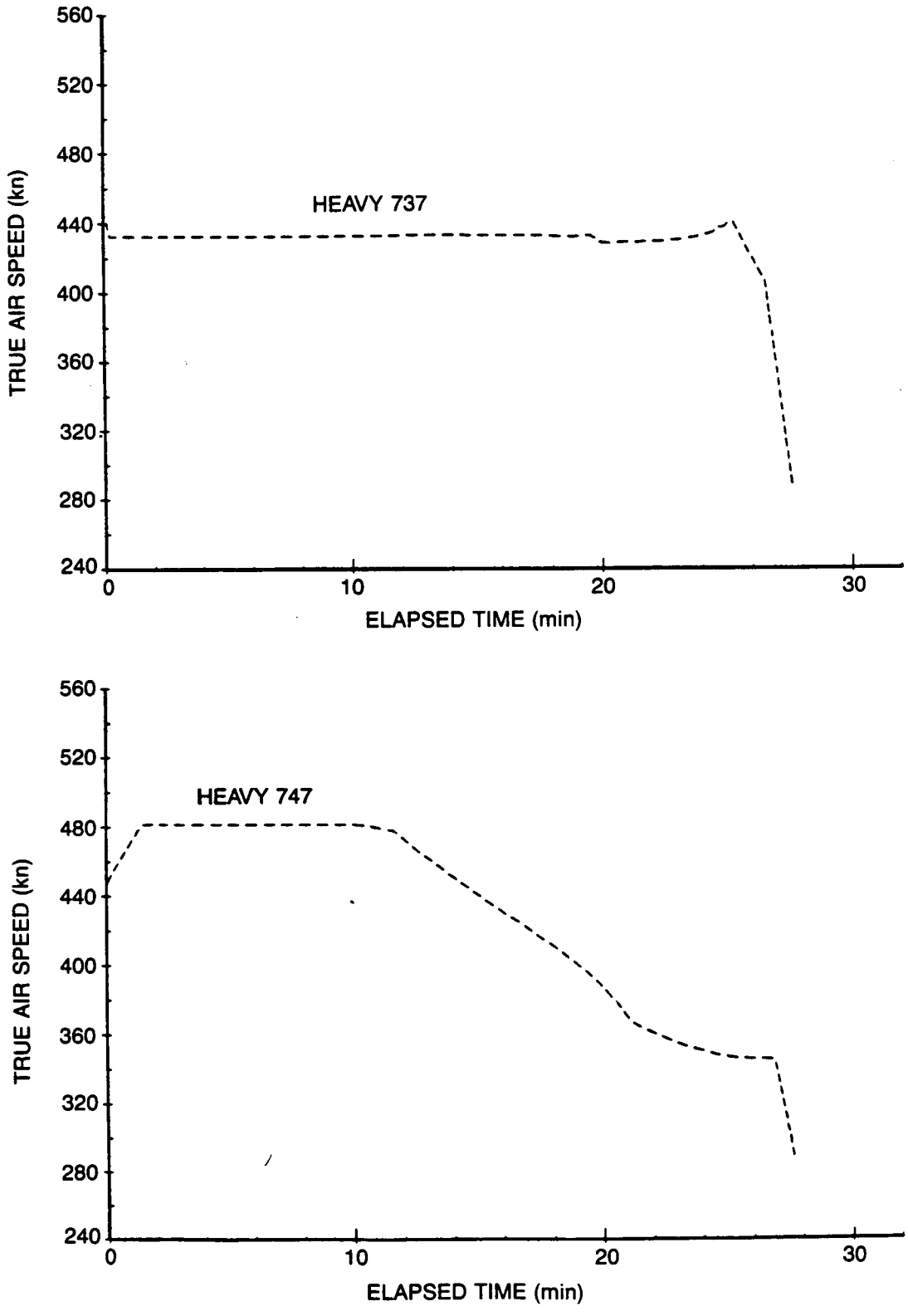

Figure 9. Descent Speed Profiles, Optimal Strategy, 1658 sec

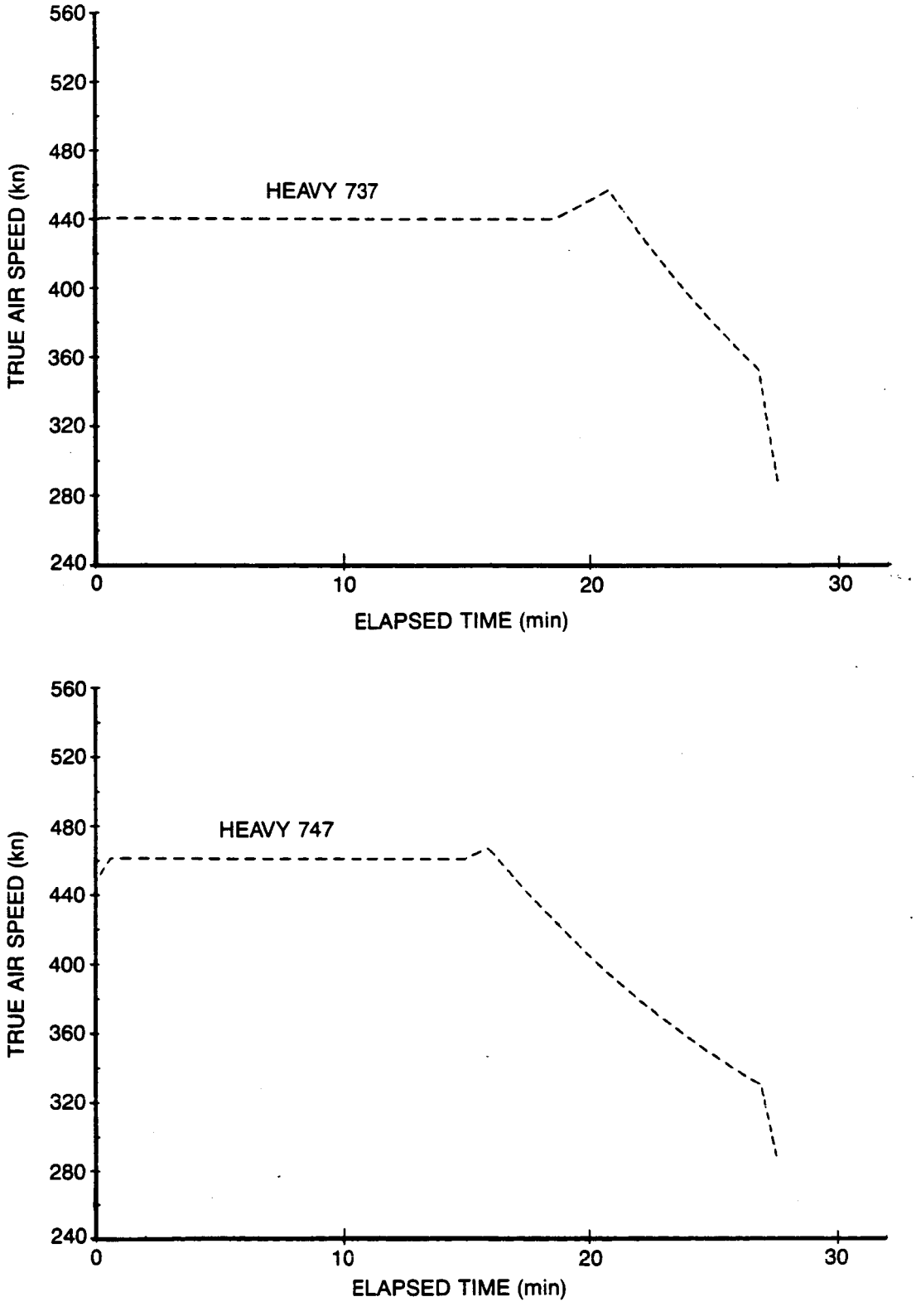

Figure 10. Descent Speed Profiles, Clean-Idle Strategy, 1658 sec

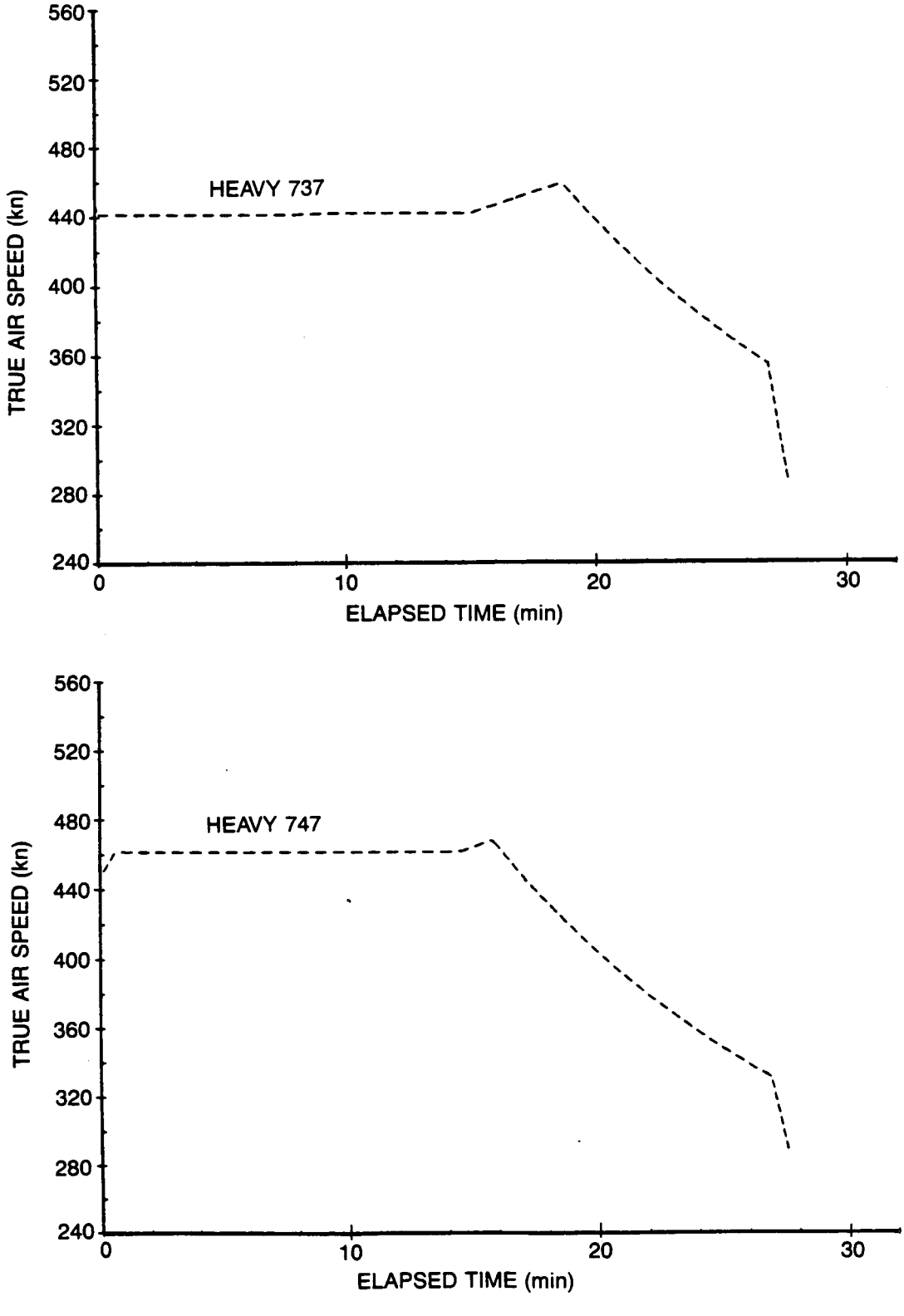

Figure 11. Descent Speed Profiles, CFPA Strategy, 1658 sec

Table 4. Minimum Time Separations (min)

AIRPLANE PAIR		1658 sec			1739 sec			1819 sec		
Lead	Trail	Opt	C-I	CFPA	Opt	C-I	CFPA	Opt	C-I	CFPA
737H	737H	1.039	1.039	1.039	1.039	1.039	1.039	1.039	1.039	1.039
737H	737L	1.054	1.041	1.050	1.074	1.053	1.047	1.048	1.042	1.041
737H	747H	1.909	1.347	1.363	1.965	1.477	1.448	1.879	1.592	1.491
737H	747L	1.977	1.050	1.075	1.935	1.107	1.058	1.760	1.128	1.037
737H	767H	1.326	1.049	1.061	1.304	1.041	1.041	1.247	1.045	1.040
737H	767L	1.124	1.047	1.051	1.075	1.045	1.034	1.037	1.043	1.034
737L	737H	1.024	1.036	1.027	1.003	1.024	1.030	1.029	1.035	1.036
737L	737L	1.039	1.039	1.039	1.039	1.039	1.039	1.039	1.039	1.039
737L	747H	1.899	1.366	1.364	1.976	1.494	1.447	1.983	1.615	1.491
737L	747L	1.965	1.072	1.076	2.002	1.127	1.057	1.880	1.152	1.037
737L	767H	1.313	1.047	1.049	1.377	1.026	1.032	1.387	1.041	1.038
737L	767L	1.109	1.044	1.040	1.153	1.030	1.025	1.146	1.040	1.032
747H	737H	0.999	1.036	1.013	0.971	1.086	1.070	0.978	1.090	1.057
747H	737L	1.014	1.038	1.025	1.006	1.101	1.079	0.987	1.093	1.059
747H	747H	1.039	1.039	1.039	1.041	1.039	1.039	1.199	1.046	1.048
747H	747L	1.064	1.014	1.045	0.983	1.088	1.082	1.123	1.084	1.054
747H	767H	1.034	1.046	1.035	1.007	1.088	1.073	0.988	1.096	1.059
747H	767L	1.025	1.044	1.026	0.974	1.092	1.066	0.977	1.094	1.052
747L	737H	0.973	1.060	1.006	1.027	1.037	1.027	1.023	1.044	1.041
747L	737L	0.988	1.063	1.018	1.062	1.052	1.036	1.032	1.048	1.043
747L	747H	1.013	1.063	1.032	1.137	1.138	1.075	1.223	1.205	1.041
747L	747L	1.039	1.039	1.039	1.039	1.039	1.039	1.147	1.039	1.039
747L	767H	1.008	1.070	1.028	1.063	1.039	1.030	1.032	1.050	1.043
747L	767L	1.000	1.068	1.019	1.030	1.043	1.023	1.022	1.049	1.037
767H	737H	1.004	1.028	1.016	1.002	1.036	1.036	1.030	1.033	1.037
767H	737L	1.019	1.031	1.028	1.037	1.051	1.045	1.039	1.036	1.039
767H	747H	1.474	1.225	1.230	1.575	1.339	1.355	1.596	1.395	1.425
767H	747L	1.392	1.007	1.049	1.362	1.038	1.047	1.382	1.027	1.034
767H	767H	1.039	1.039	1.039	1.039	1.039	1.039	1.039	1.039	1.039
767H	767L	1.030	1.036	1.029	1.005	1.043	1.032	1.028	1.037	1.032
767L	737H	1.012	1.030	1.026	1.035	1.032	1.043	1.040	1.034	1.043
767L	737L	1.027	1.033	1.038	1.071	1.047	1.052	1.049	1.038	1.045
767L	747H	1.594	1.303	1.248	1.682	1.416	1.364	1.764	1.463	1.429
767L	747L	1.609	1.009	1.059	1.603	1.034	1.054	1.627	1.029	1.041
767L	767H	1.047	1.041	1.048	1.072	1.034	1.046	1.173	1.040	1.045
767L	767L	1.039	1.039	1.039	1.039	1.039	1.039	1.039	1.039	1.039

Table 5. Maximum Flow Rates (ACPH)

AIRPLANE PAIR		1658 sec			1739 sec			1819 sec		
Lead	Trail	Opt	C-I	CFPA	Opt	C-I	CFPA	Opt	C-I	CFPA
737H	737H	57.77	57.77	57.77	57.77	57.77	57.77	57.77	57.77	57.77
737H	737L	56.80	57.73	57.99	57.74	57.67	57.72	57.25	58.47	57.76
737H	747H	31.54	44.50	44.40	30.47	40.26	41.23	32.09	37.44	40.08
737H	747L	30.52	56.46	56.65	30.58	54.21	56.93	34.09	53.21	57.01
737H	767H	45.63	57.55	57.81	46.02	57.67	57.68	48.13	58.40	57.69
737H	767L	54.01	57.58	57.95	55.82	57.63	57.12	57.84	58.41	57.12
737L	737H	58.77	57.81	57.55	57.80	57.87	57.82	58.30	57.08	57.78
737L	737L	57.77	57.77	57.77	57.77	57.77	57.77	57.77	57.77	57.77
737L	747H	31.72	43.86	44.14	30.33	39.66	41.16	30.39	36.79	40.06
737L	747L	30.71	55.30	56.19	29.58	52.99	56.79	31.91	51.82	57.01
737L	767H	46.11	57.58	57.59	43.57	57.78	57.74	43.26	57.70	57.70
737L	767L	54.81	57.61	57.73	51.98	57.73	57.17	52.34	57.71	57.12
747H	737H	58.17	57.50	57.50	58.34	57.62	56.94	58.76	56.46	57.66
747H	737L	57.18	57.47	57.72	58.31	57.52	56.89	58.23	57.13	57.66
747H	747H	57.77	57.77	57.77	57.59	57.77	57.77	49.10	57.40	57.26
747H	747L	57.31	57.23	57.44	57.24	57.60	56.79	50.59	56.76	56.91
747H	767H	58.05	57.29	57.54	58.24	57.52	56.85	57.41	57.06	57.59
747H	767L	57.78	57.31	57.68	58.37	57.48	56.30	58.84	57.08	57.01
747L	737H	58.64	58.05	57.84	58.89	57.79	57.93	58.65	57.47	58.55
747L	737L	57.64	58.01	58.06	58.86	57.69	57.87	58.12	58.16	58.55
747L	747H	58.24	57.72	58.11	55.22	51.93	55.21	50.77	49.31	51.41
747L	747L	57.77	57.77	57.77	57.77	57.77	57.77	52.32	57.77	57.77
747L	767H	58.52	57.83	57.88	58.78	57.70	57.84	58.14	58.09	58.47
747L	767L	58.25	57.85	58.02	58.91	57.65	57.27	58.72	58.10	57.88
767H	737H	57.89	57.99	57.73	57.87	57.87	57.86	58.27	57.16	57.85
767H	737L	56.91	57.96	57.95	57.84	57.76	57.80	57.75	57.84	57.84
767H	747H	40.71	48.83	48.80	38.32	44.26	44.01	38.20	42.47	41.91
767H	747L	43.21	57.71	57.66	43.04	57.84	57.70	43.40	57.45	57.08
767H	767H	57.77	57.77	57.77	57.77	57.77	57.77	57.77	57.77	57.77
767H	767L	57.51	57.80	57.91	57.90	57.72	57.20	58.34	57.78	57.19
767L	737H	58.15	57.97	57.59	57.75	57.92	58.44	57.70	57.14	58.44
767L	737L	57.17	57.93	57.81	57.71	57.81	58.39	57.18	57.83	58.43
767L	747H	37.63	45.98	48.24	35.61	41.82	43.98	34.61	40.50	42.00
767L	747L	37.34	57.69	57.52	36.81	57.89	58.28	36.87	57.44	57.66
767L	767H	58.03	57.74	57.63	57.56	57.82	58.35	51.16	57.76	58.36
767L	767L	57.77	57.77	57.77	57.77	57.77	57.77	57.77	57.77	57.77

Table 6. Throughput Reduction Due to Increasing B747 Levels

ELAPSED TIME (sec)	STRATEGY	B747 = 0% B737 = 50% B767 = 50%	B747 = 40% B737 = 30% B767 = 30%	REDUCTION (PERCENT)
	Clean-Idle	57.77	56.17	-2.77
1658	CFPA	57.77	56.32	-2.51
	Optimal	55.80	51.76	-7.24
	Clean-Idle	57.77	55.30	-4.28
1739	CFPA	57.77	55.64	-3.69
	Optimal	55.67	51.46	-7.56
	Clean-Idle	57.77	54.75	-5.23
1819	CFPA	57.77	55.42	-4.07
	Optimal	55.54	50.56	-8.97

ELAPSED TIME (sec)	STRATEGY	B747 = 0% B737 = 100% B767 = 0%	B747 = 50% B737 = 50% B767 = 0%	REDUCTION (PERCENT)
	Clean-Idle	57.77	55.80	-3.41
1658	CFPA	57.77	55.92	-3.20
	Optimal	57.78	51.15	-11.47
	Clean-Idle	57.77	54.62	-5.45
1739	CFPA	57.77	55.27	-4.33
	Optimal	57.77	50.89	-11.91
	Clean-Idle	57.77	53.80	-6.87
1819	CFPA	57.77	55.06	-4.69
	Optimal	57.77	49.76	-13.87

Table 7. Best Achievable Throughputs for Given Strategy and Elapsed Time

ELAPSED TIME (sec)	STRATEGY	THROUGHPUT (ACPH)	CONDITIONS
1658	Clean-Idle	57.77	B747=0%, any mix B737/B767
	CFPA	57.77	B747=0%, any mix B737/B767
	Optimal	57.77	B747=0%, all B737 or all B767
1739	Clean-Idle	57.77	B747=0%, any mix B737/B767
	CFPA	57.77	B747=0%, any mix B737/B767
	Optimal	57.77	B747=0%, B737=100%, B767=0%
1819	Clean-Idle	57.77	B747=0%, any mix B737/B767
	CFPA	57.77	B747=0%, any mix B737/B767
	Optimal	57.77	B747=0%, B737=100%, B767=0%

Table 8. Worst Achievable Throughputs for Given Strategy and Elapsed Time

ELAPSED TIME (sec)	STRATEGY	THROUGHPUT (ACPH)	REDUCTION FROM BEST (PERCENT)	CONDITIONS
1658	Clean-Idle	55.80	-3.41	B767=0%, B737=50%, B747=50%
	CFPA	55.92	-3.20	B767=0%, B737=50%, B747=50%
	Optimal	51.15	-11.46	B767=0%, B737=50%, B747=50%
1739	Clean-Idle	54.56	-5.56	B767=0%, B737=40%, B747=60%
	CFPA	55.27	-4.33	B767=0%, B737=50%, B747=50%
	Optimal	50.89	-11.91	B767=0%, B737=50%, B747=50%
1819	Clean-Idle	53.66	-7.11	B767=0%, B737=40%, B747=60%
	CFPA	54.94	-4.90	B767=0%, B737=40%, B747=60%
	Optimal	49.06	-15.08	B767=0%, B737=30%, B747=70%

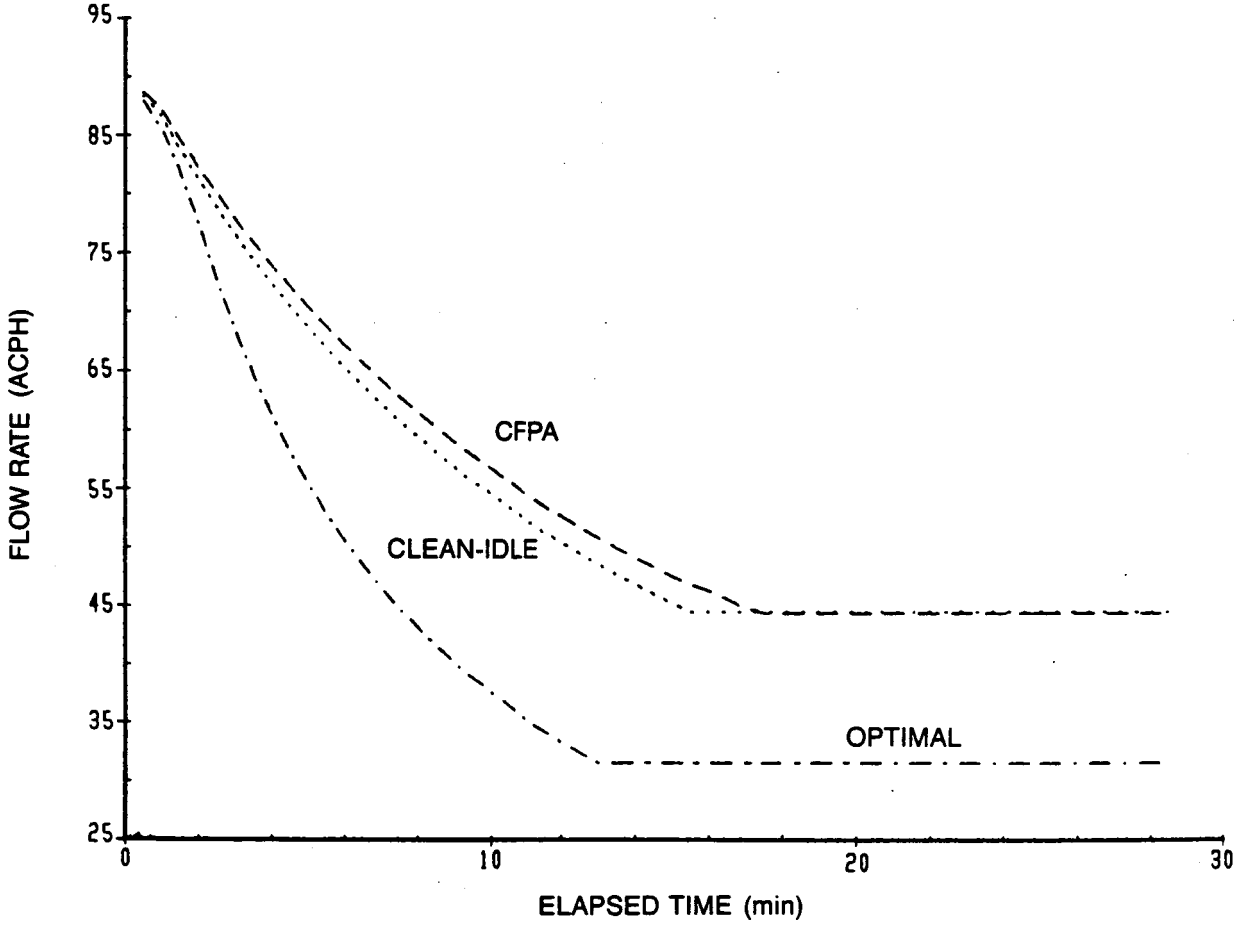

Figure 12. Flow Rate Degradation—Heavy B737 Followed by Heavy B747, Elapsed Time = 1658 sec

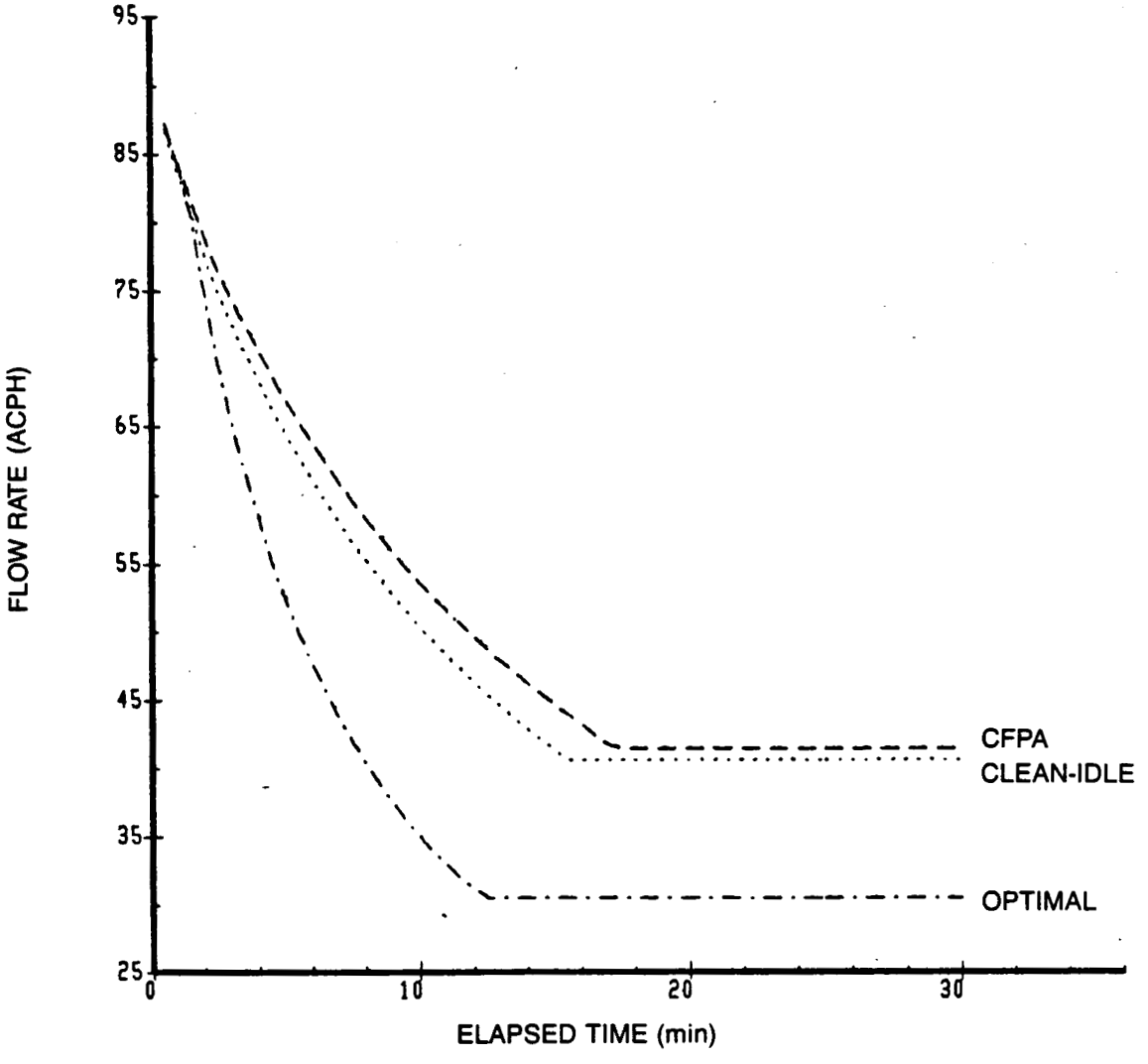

Figure 13. Flow Rate Degradation—Heavy B737 Followed by Heavy B747, Elapsed Time = 1739 sec

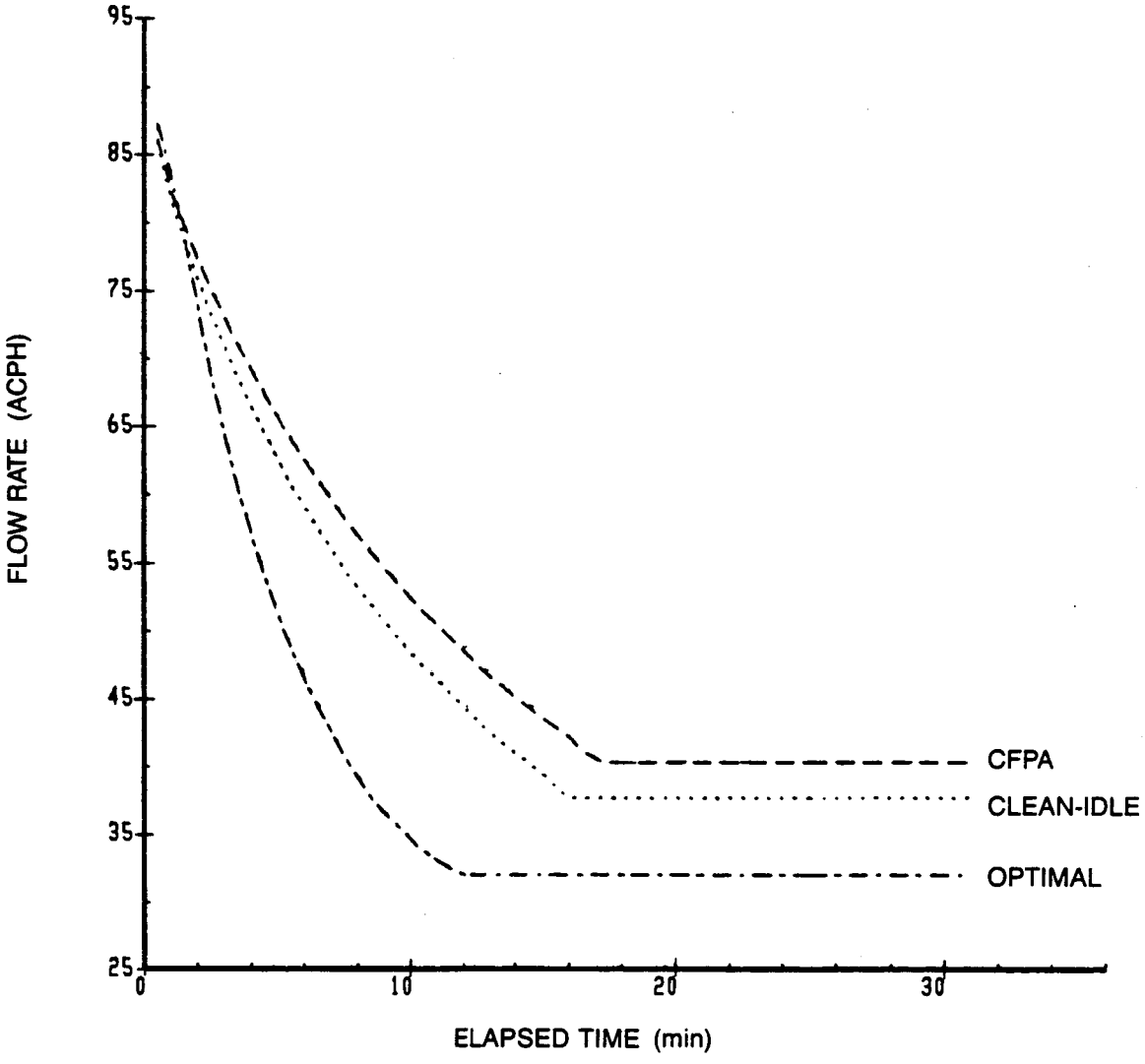

Figure 14. Flow Rate Degradation—Heavy B737 Followed by Heavy B747, Elapsed Time = 1819 sec

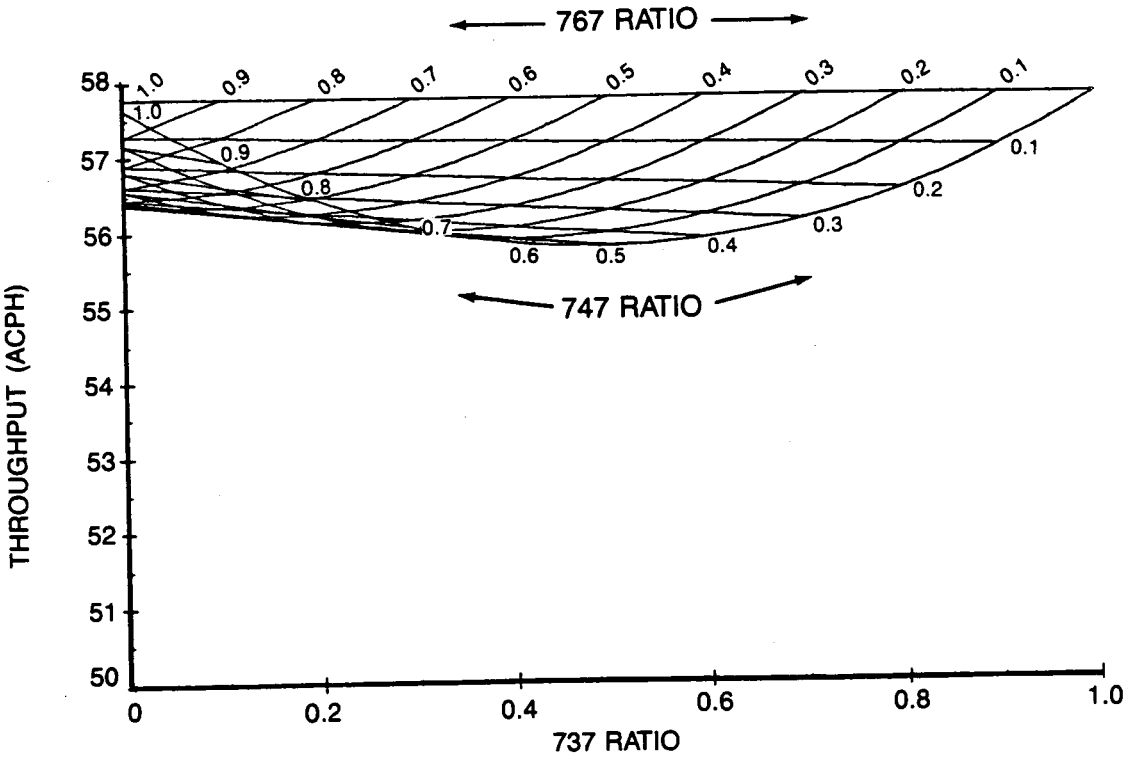

Figure 15. Mixed Traffic Throughput, Clean-Idle Strategy, Elapsed Time = 1658 sec

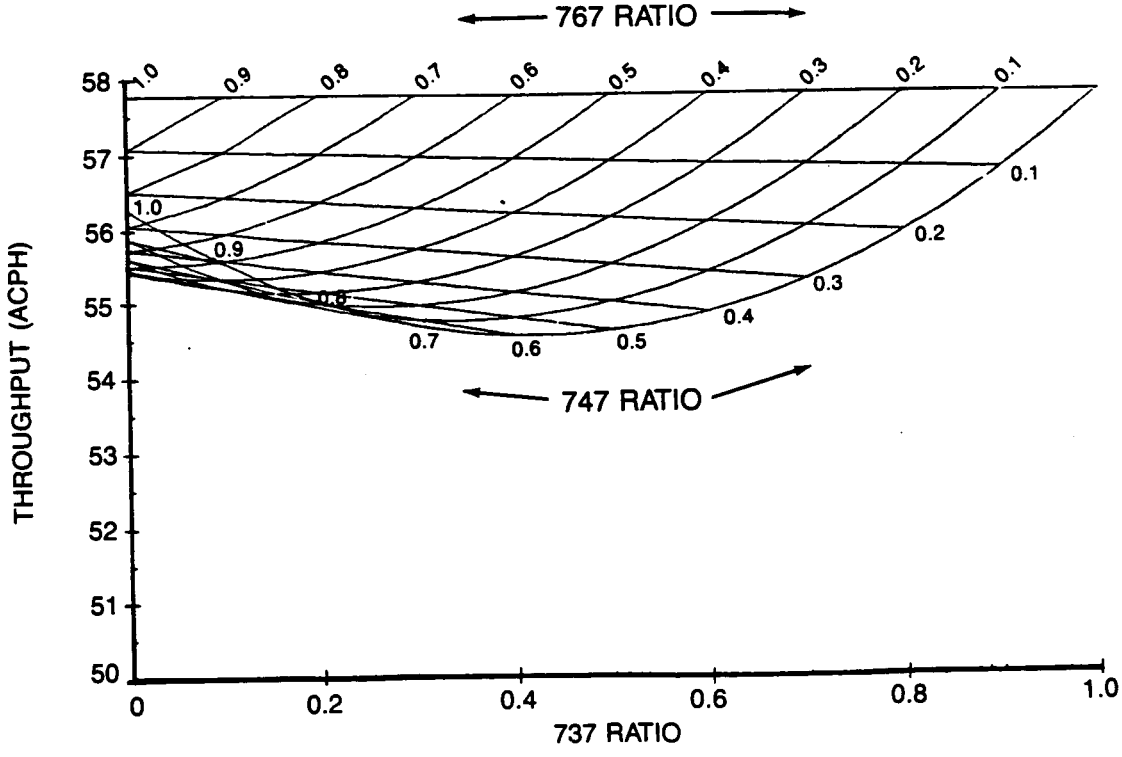

Figure 16. Mixed Traffic Throughput, Clean-Idle Strategy, Elapsed Time = 1739 sec

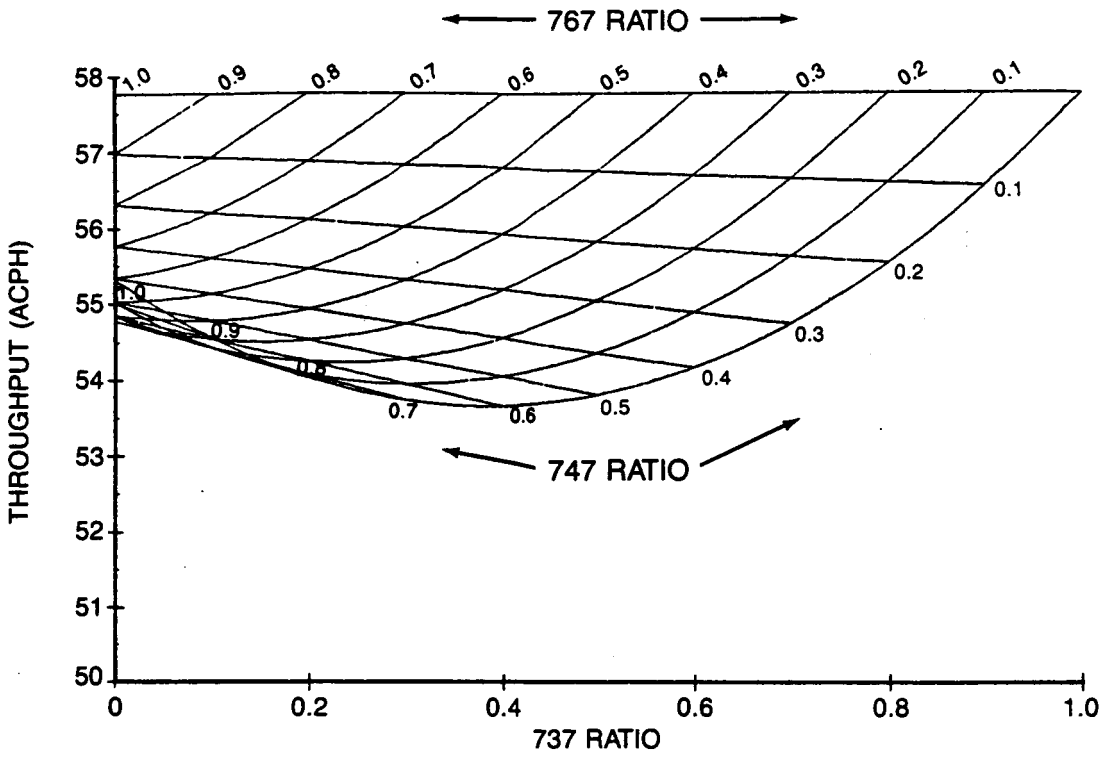

Figure 17. Mixed Traffic Throughput, Clean-Idle Strategy, Elapsed Time = 1819 sec

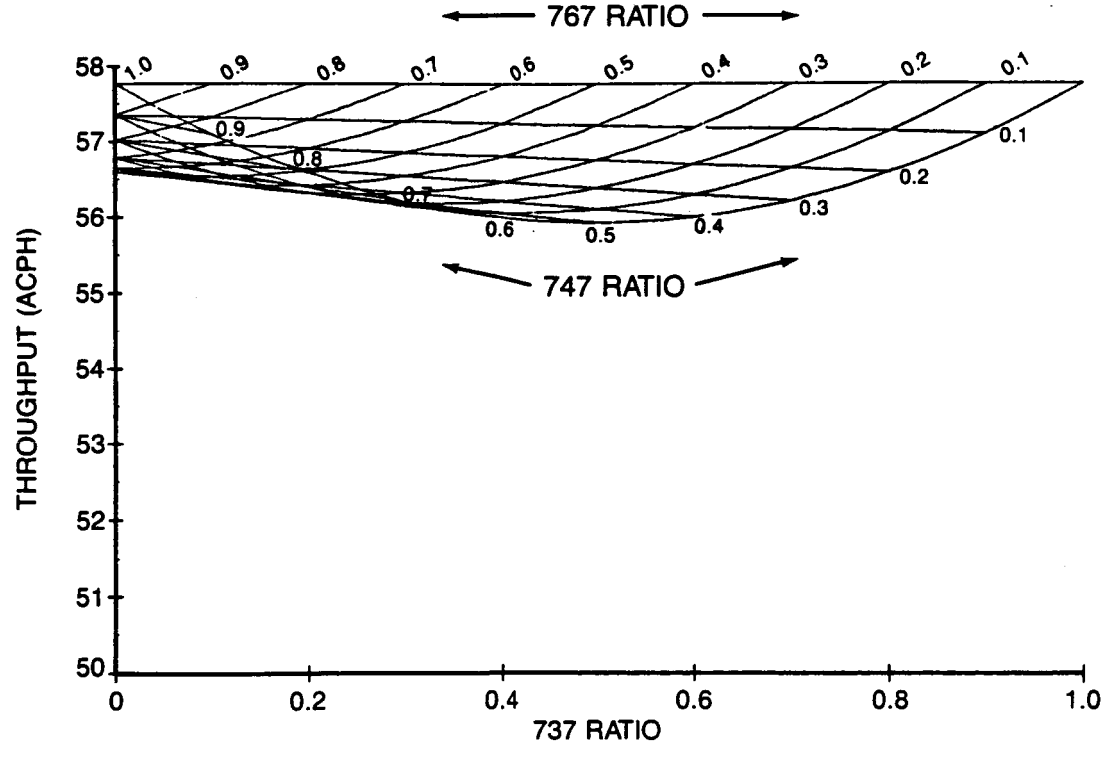

Figure 18. Mixed Traffic Throughput, CFPA Strategy, Elapsed Time = 1658 sec

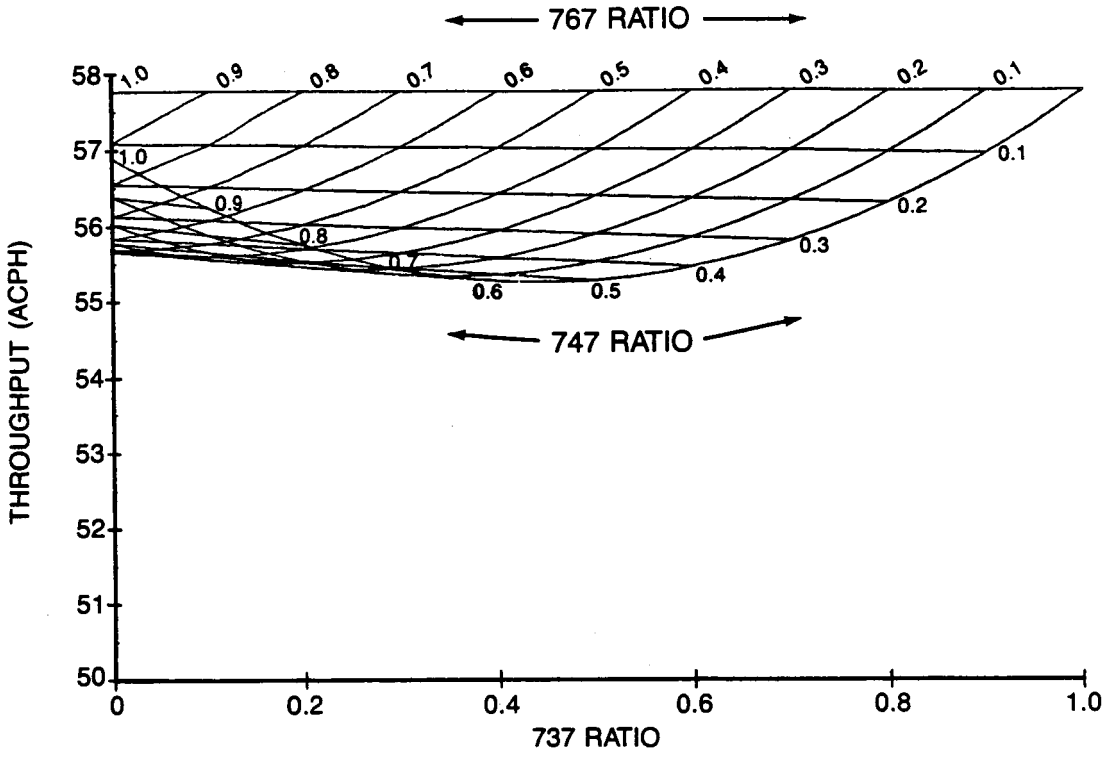

Figure 19. Mixed Traffic Throughput, CFPA Strategy, Elapsed Time = 1739 sec

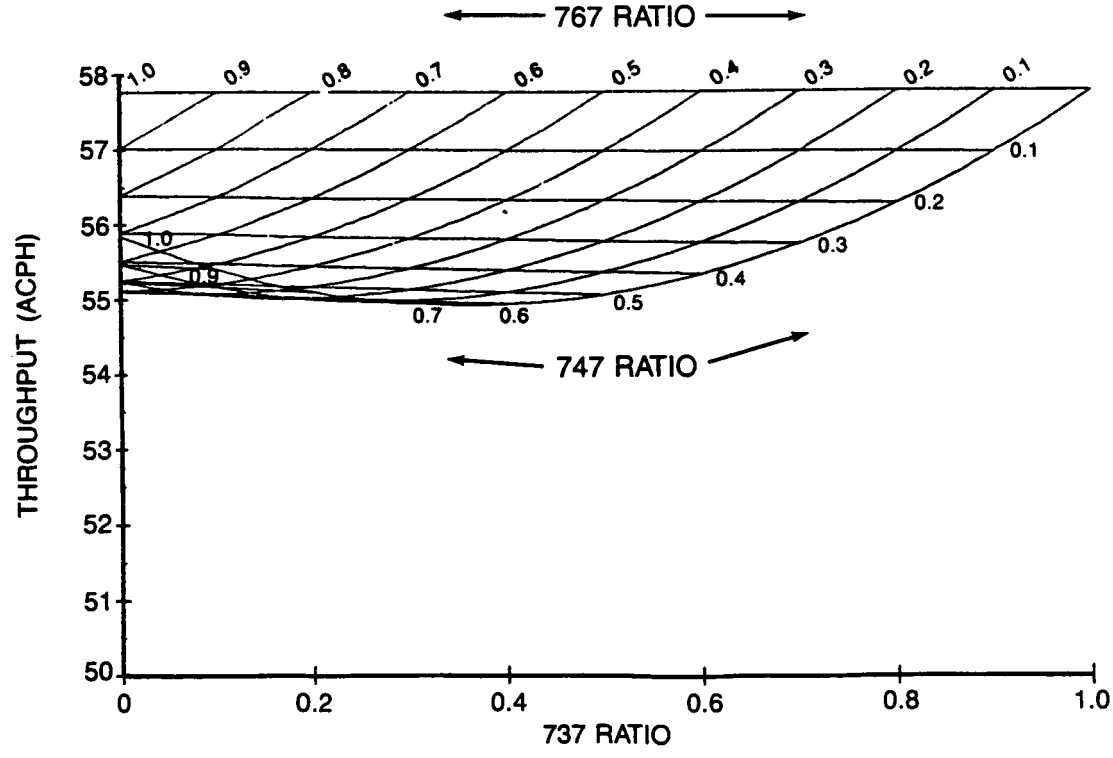

Figure 20. Mixed Traffic Throughput, CFPA Strategy, Elapsed Time = 1819 sec

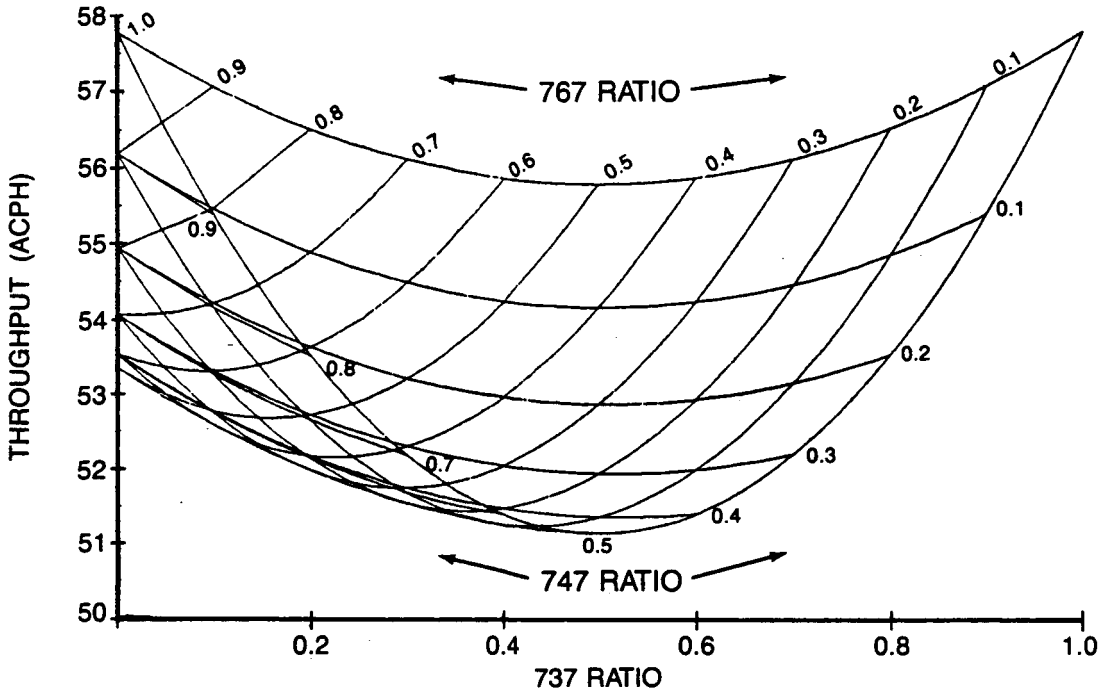

Figure 21. Mixed Traffic Throughput, Optimal Strategy, Elapsed Time = 1658 sec

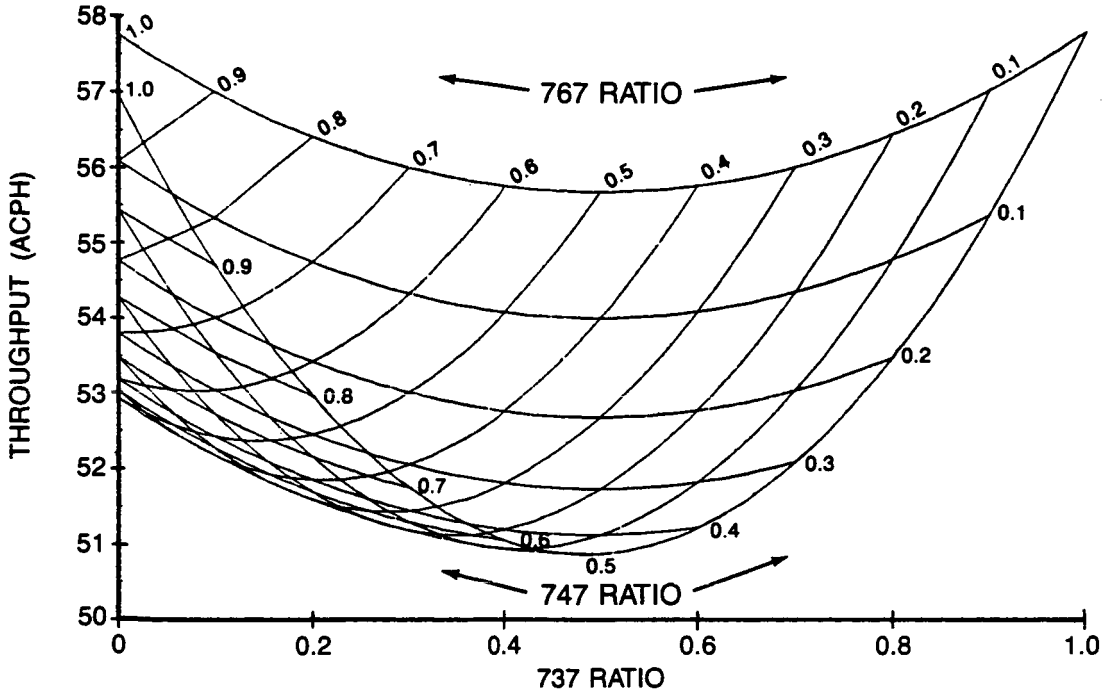

Figure 22. Mixed Traffic Throughput, Optimal Strategy, Elapsed Time = 1739 sec

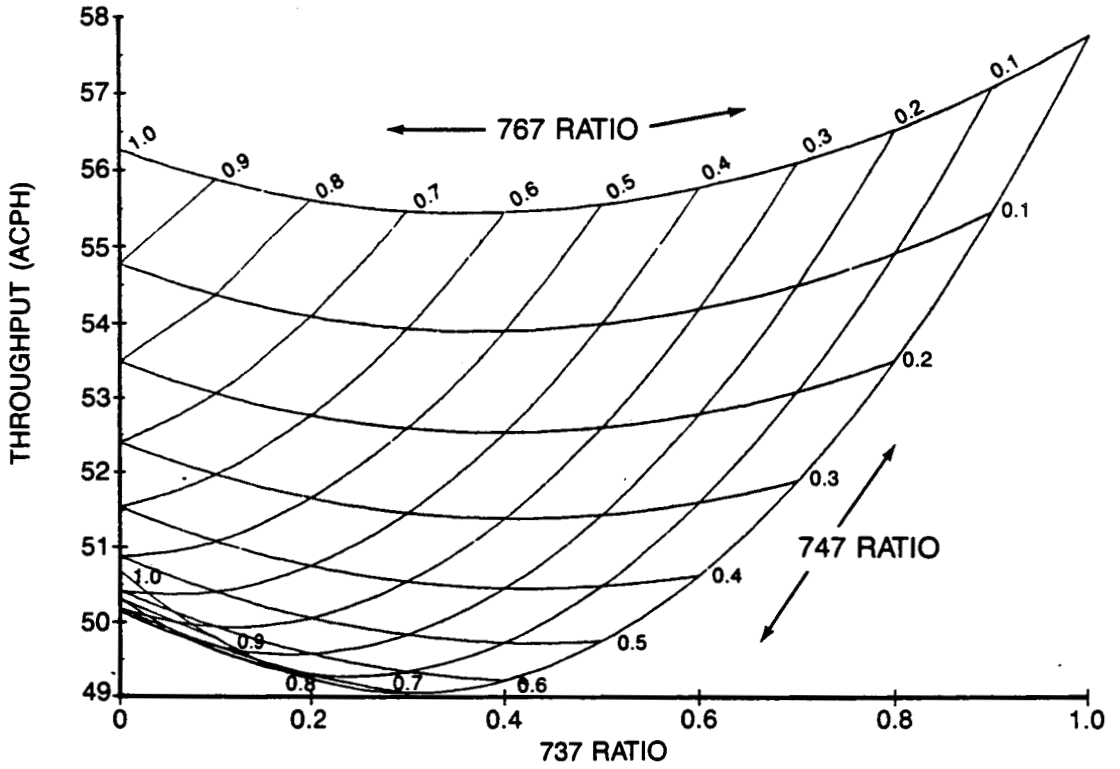

Figure 23. Mixed Traffic Throughput, Optimal Strategy, Elapsed Time = 1819 sec

Table 9. Probabilities of Airplane Pairs at a Typical ERM Airport

Airplane Type	AIRPLANE TYPE	B737		B767		B747	
	Weight	Light	Heavy	Light	Heavy	Light	Heavy
B737	Light	0.19329	0.19329	0.01064	0.01064	0.01590	0.01590
	Heavy	0.19329	0.19329	0.01064	0.01064	0.01590	0.01590
B767	Light	0.01064	0.01064	0.00059	0.00059	0.00087	0.00087
	Heavy	0.01064	0.01064	0.00059	0.00059	0.00087	0.00087
B747	Light	0.01590	0.01590	0.00087	0.00087	0.00131	0.00131
	Heavy	0.01590	0.01590	0.00087	0.00087	0.00131	0.00131

Table 10. Throughput and Fuel Use at a Typical ERM Airport

ELAPSED TIME (sec)	STRATEGY	THROUGHPUT (ACPH)	STANDARD DEVIATION, THROUGHPUT (ACPH)	FUEL USE (lb PER AIRPLANE
	Clean-Idle	57.26	2.44	1850.1
1658	CFPA	57.28	2.41	1917.1
	Optimal	55.69	6.76	1812.4
	Clean-Idle	57.03	3.25	1750.2
1739	CFPA	57.16	2.96	1791.8
	Optimal	55.65	7.01	1733.1
	Clean-Idle	56.88	3.80	1718.0
1819	CFPA	57.17	3.19	1748.2
	Optimal	55.76	6.58	1690.6

Table 11. Average Throughput and Minimum Time Separation Data for the B737-300 Type in Typical Traffic

STRATEGY	ELAPSED TIME (sec)	AVERAGE THROUGHPUT (ACPH)	AVERAGE MINIMUM TIME SEPARATION (min)
Optimal	1658	57.78	1.038
	1739	57.81	1.038
	1819	57.77	1.039
Clean-Idle	1658	57.77	1.039
	1739	57.78	1.038
	1819	57.77	1.039
CFPA	1658	57.78	1.038
	1739	57.77	1.039
	1819	57.77	1.039

Table 12. Total Fuel Usage (lb)

AIRPLANE TYPE		B737-300		B767-200		B747-200	
Delay (sec)	Strategy	Light	Heavy	Light	Heavy	Light	Heavy
1658	Clean-Idle	1459.4	1541.4	2517.5	2738.3	5320.6	5843.0
	Constant Flightpath Angle	1550.3	1593.3	2633.6	2775.0	5347.3	5830.7
	Optimal	1435.7	1510.0	2505.5	2747.4	5147.9	5645.7
1739	Clean-Idle	1365.2	1438.1	2390.2	2634.7	5178.7	5776.8
	Constant Flightpath Angle	1415.1	1468.3	2433.9	2712.7	5170.9	5880.9
	Optimal	1364.4	1431.6	2382.2	2597.4	5055.2	5547.8
1819	Clean-Idle	1326.9	1408.1	2314.9	2584.5	5134.0	5845.1
	Constant Flightpath Angle	1352.3	1421.8	2353.8	2722.1	5163.9	6059.1
	Optimal	1316.1	1387.0	2316.0	2552.8	5021.7	5610.9

Table 13. Percent Change in Descent Fuel Usage Relative to Clean-Idle Descent

AIRPLANE TYPE		B737-300		B767-200		B747-200	
Delay (sec)	Strategy	Light	Heavy	Light	Heavy	Light	Heavy
	Clean-Idle	0.00	0.00	0.00	0.00	0.00	0.00
1658	Constant Flightpath Angle	6.23	3.37	4.61	1.34	0.50	-0.21
	Optimal	-1.62	-2.04	-0.48	0.33	-3.25	-3.38
	Clean-Idle	0.00	0.00	0.00	0.00	0.00	0.00
1739	Constant Flightpath Angle	3.66	2.10	1.83	2.96	-0.15	1.80
	Optimal	-0.06	-0.45	-0.33	-1.42	-2.38	-3.96
	Clean-Idle	0.00	0.00	0.00	0.00	0.00	0.00
1819	Constant Flightpath Angle	1.91	0.97	1.68	5.32	0.58	3.66
	Optimal	-0.81	-1.50	0.05	-1.23	-2.19	-4.01

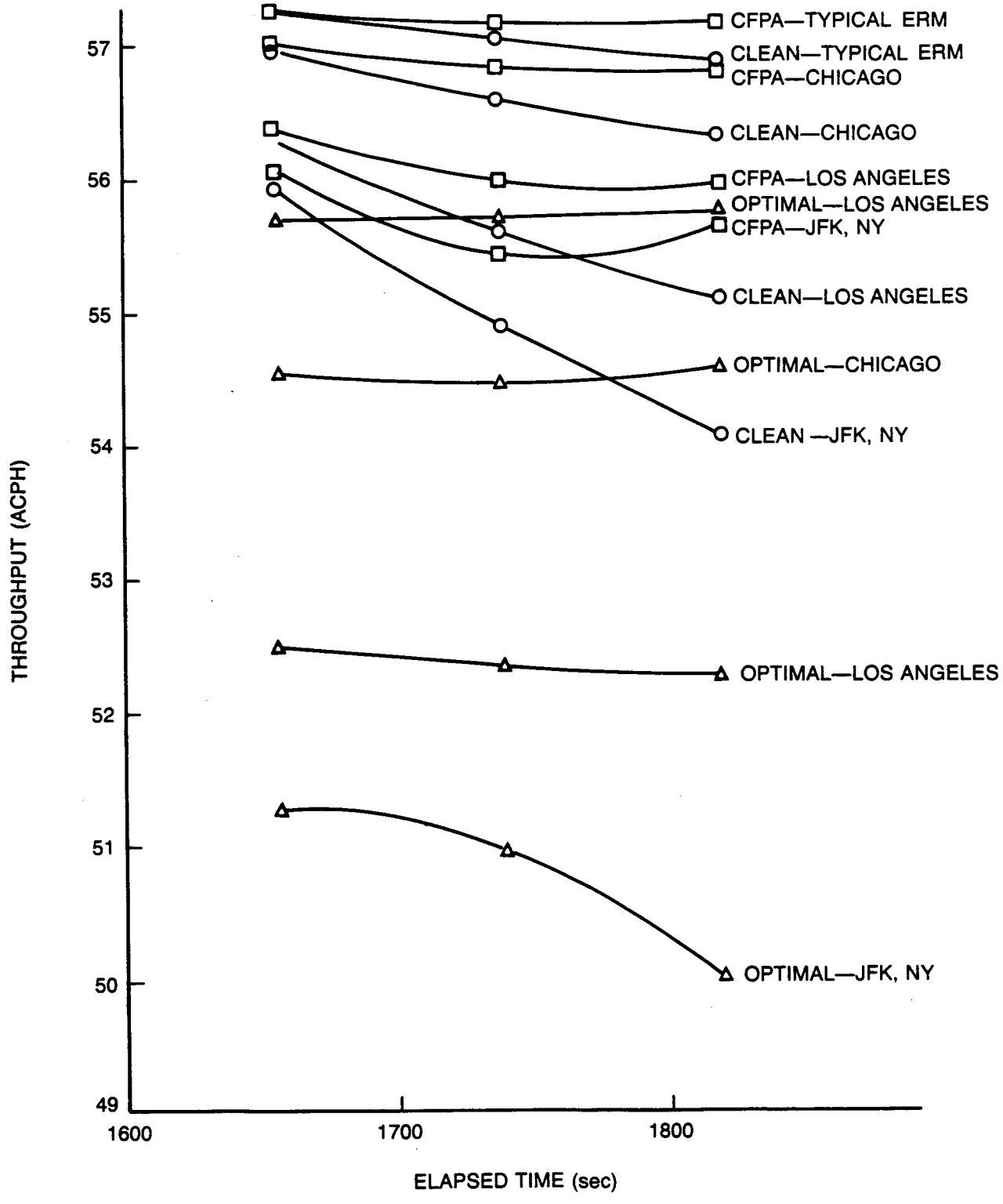

Figure 24. Throughput Performance at Various U.S. Airports

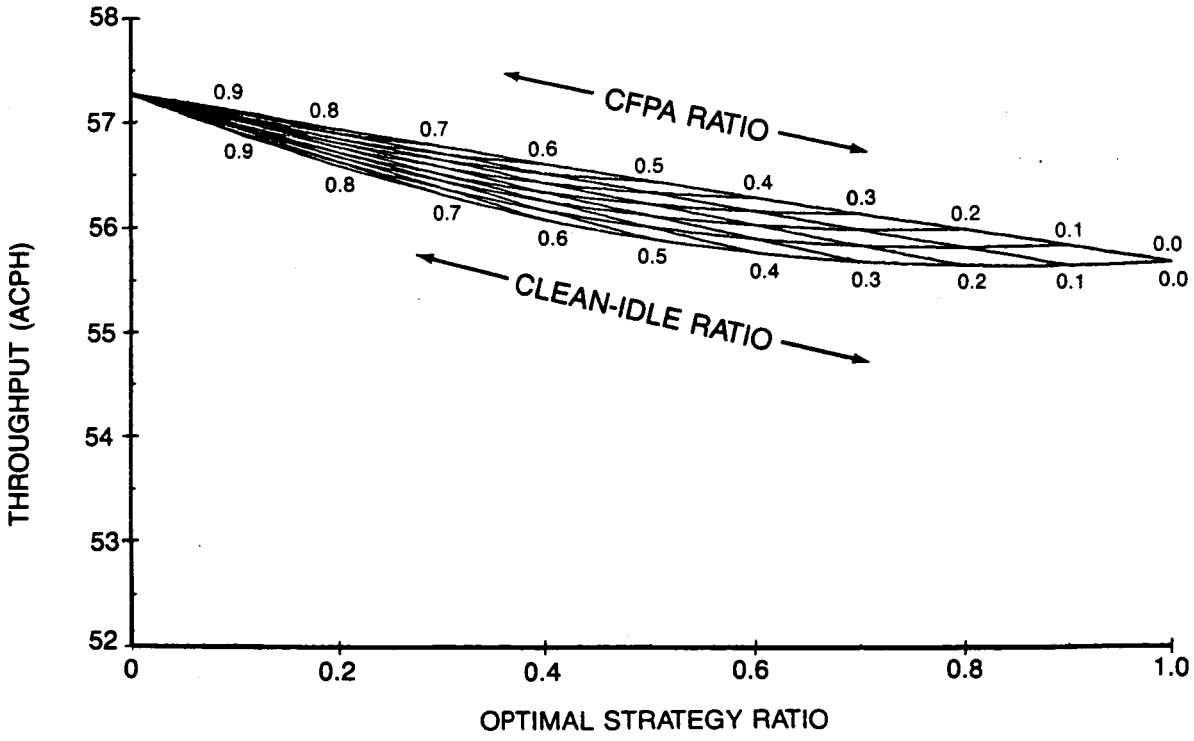

Figure 25. Mixed Strategy Throughput, Short Elapsed Time, ERM Typical Airport

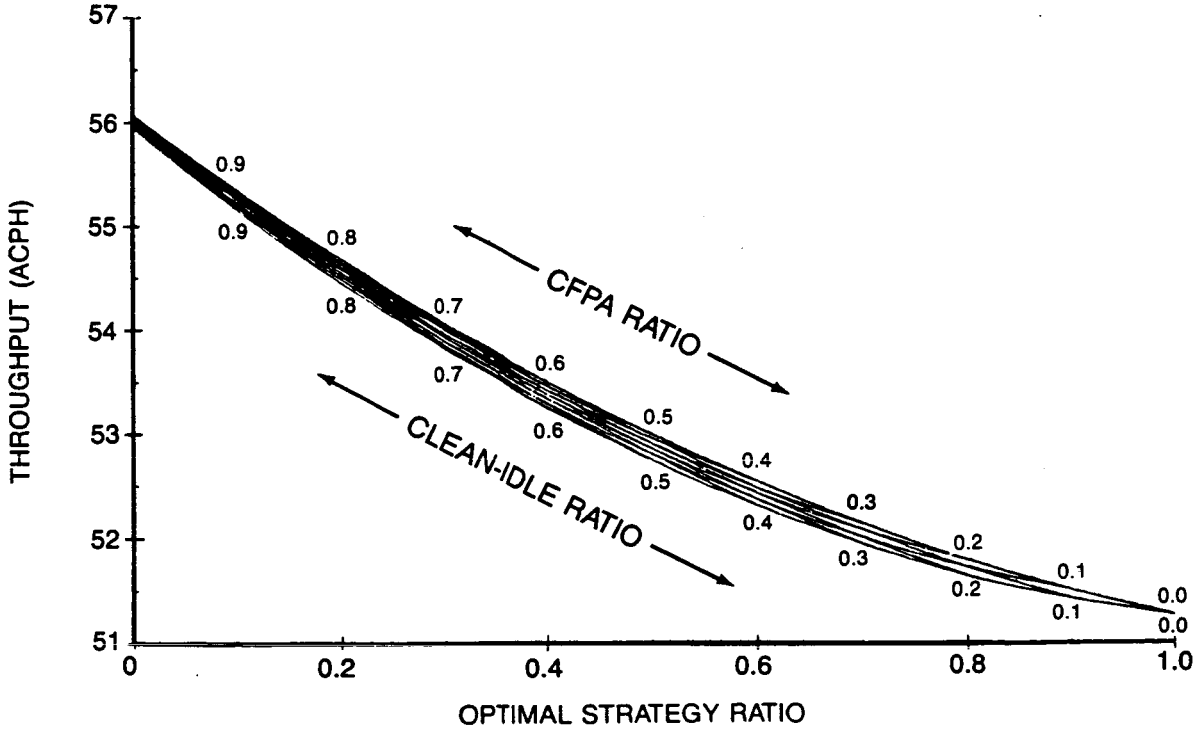

Figure 26. Mixed Strategy Throughput, Short Elapsed Time, John F. Kennedy International Airport

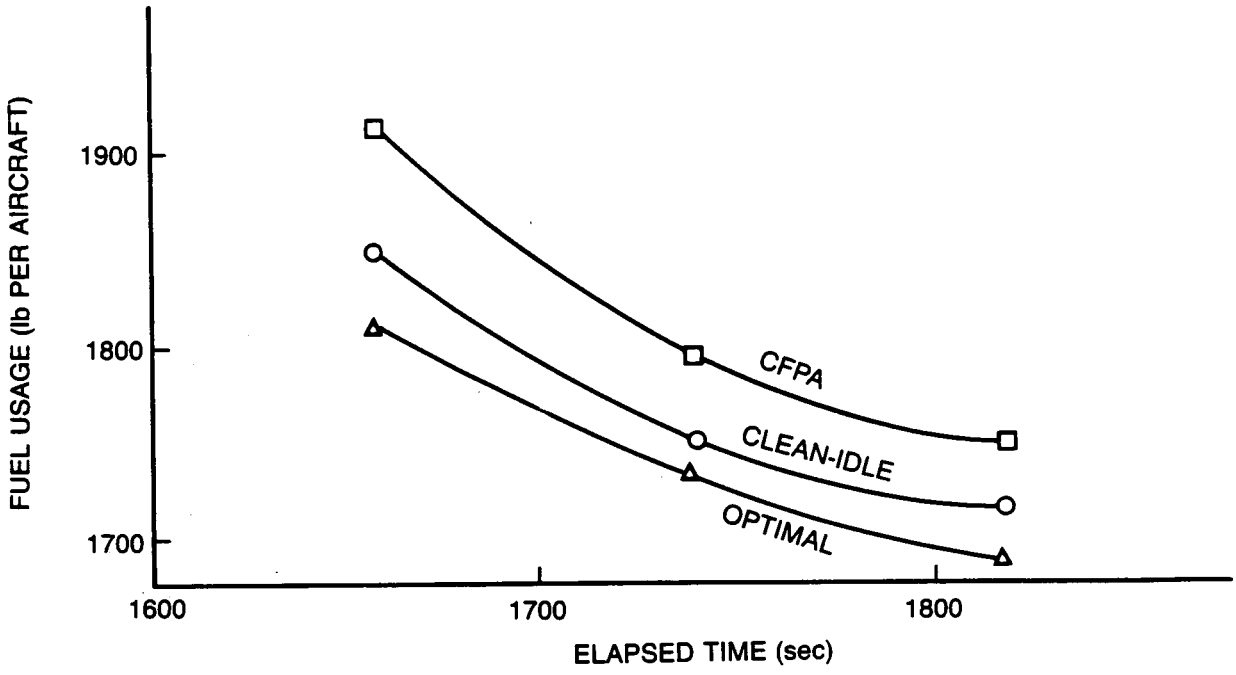

Figure 27. Fuel Versus Elapsed Time, Typical ERM Airport

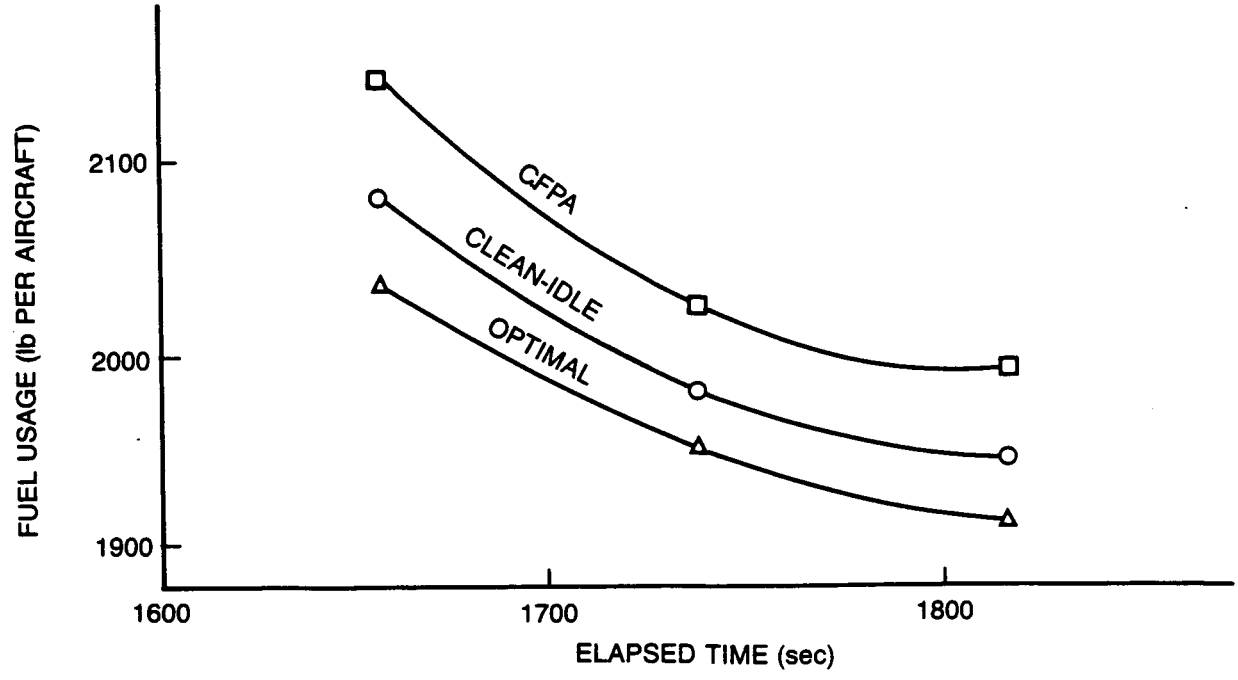

Figure 28. Fuel Versus Elapsed Time, Chicago O'Hare International Airport

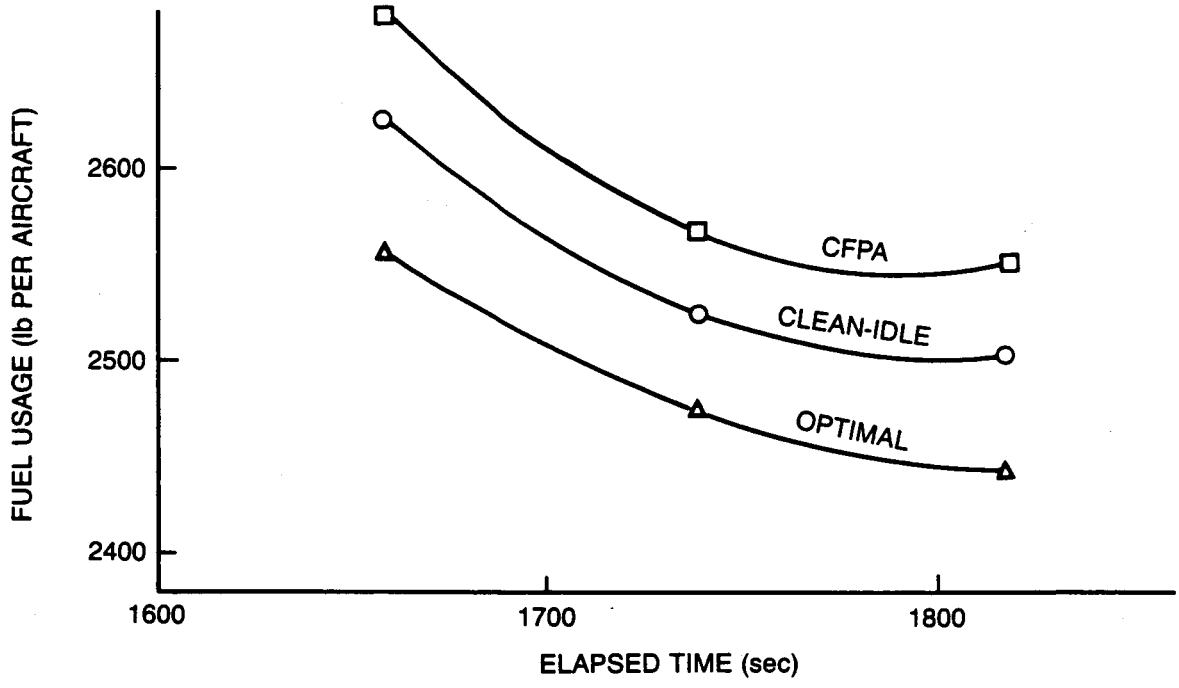

Figure 29. Fuel Versus Elapsed Time, Los Angeles International Airport

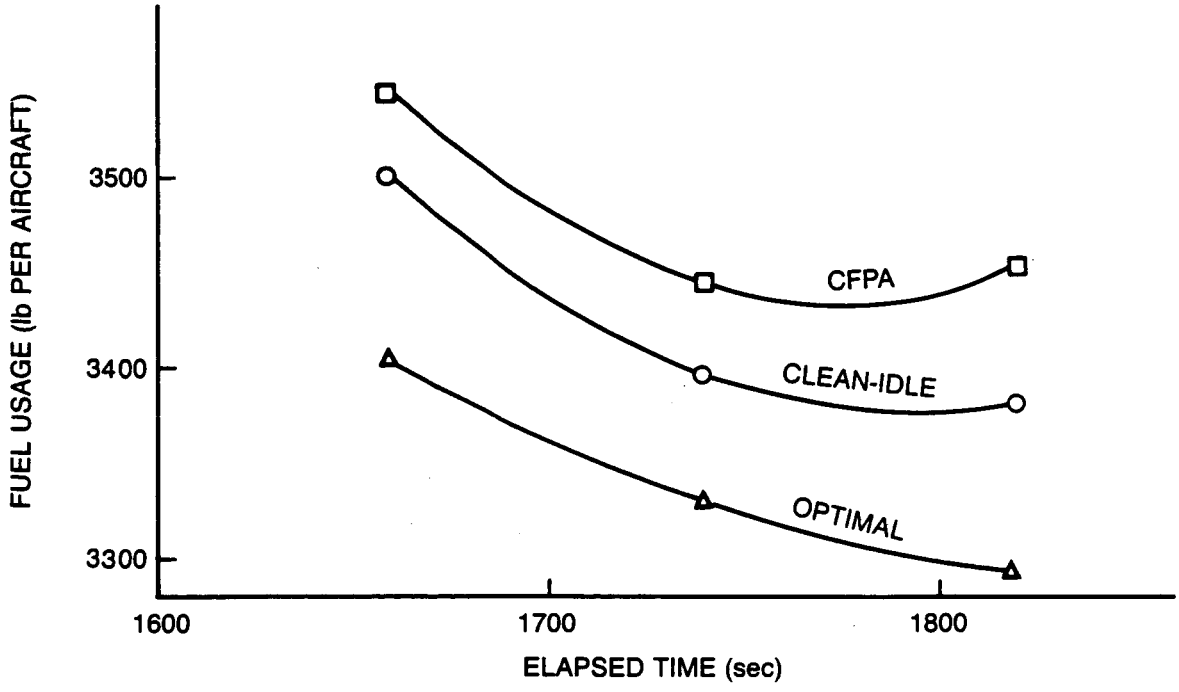

Figure 30. Fuel Versus Elapsed Time, John F. Kennedy International Airport

Table B.1. Maximum Fuel Usage and Throughput Dispersion Ratios (Standard Deviation/Mean, σ/μ)

		CFPA	CLEAN-IDLE	OPTIMAL
ERM	Fuel	0.012	0.013	0.032
	Throughput	0.002	0.002	0.006
JFK	Fuel	0.025	0.025	0.046
	Throughput	0.007	0.007	0.016

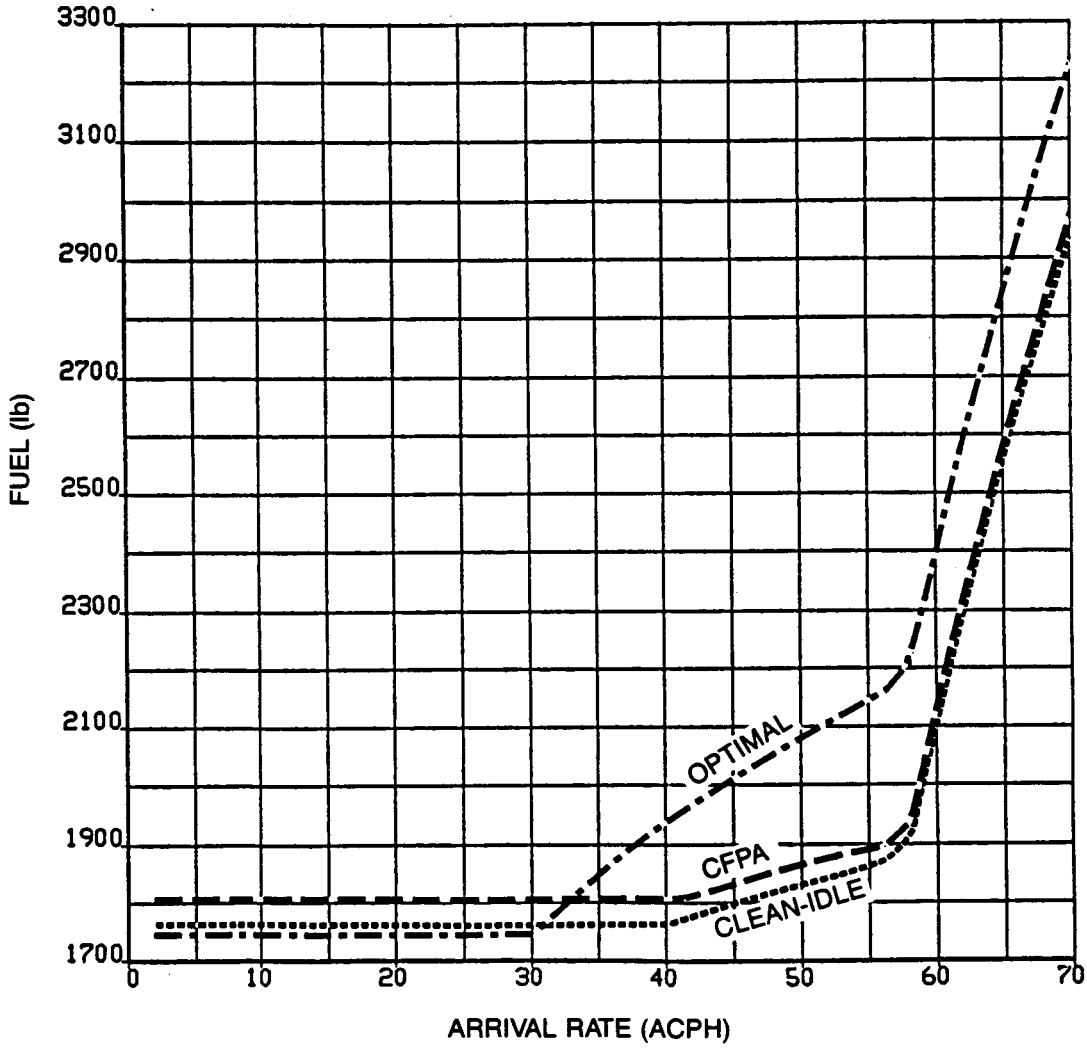

Figure B.1. Fuel Usage (Per Airplane), Typical ERM Airport Distribution (Average of 1000 Runs; 120 Airplane Pairs)

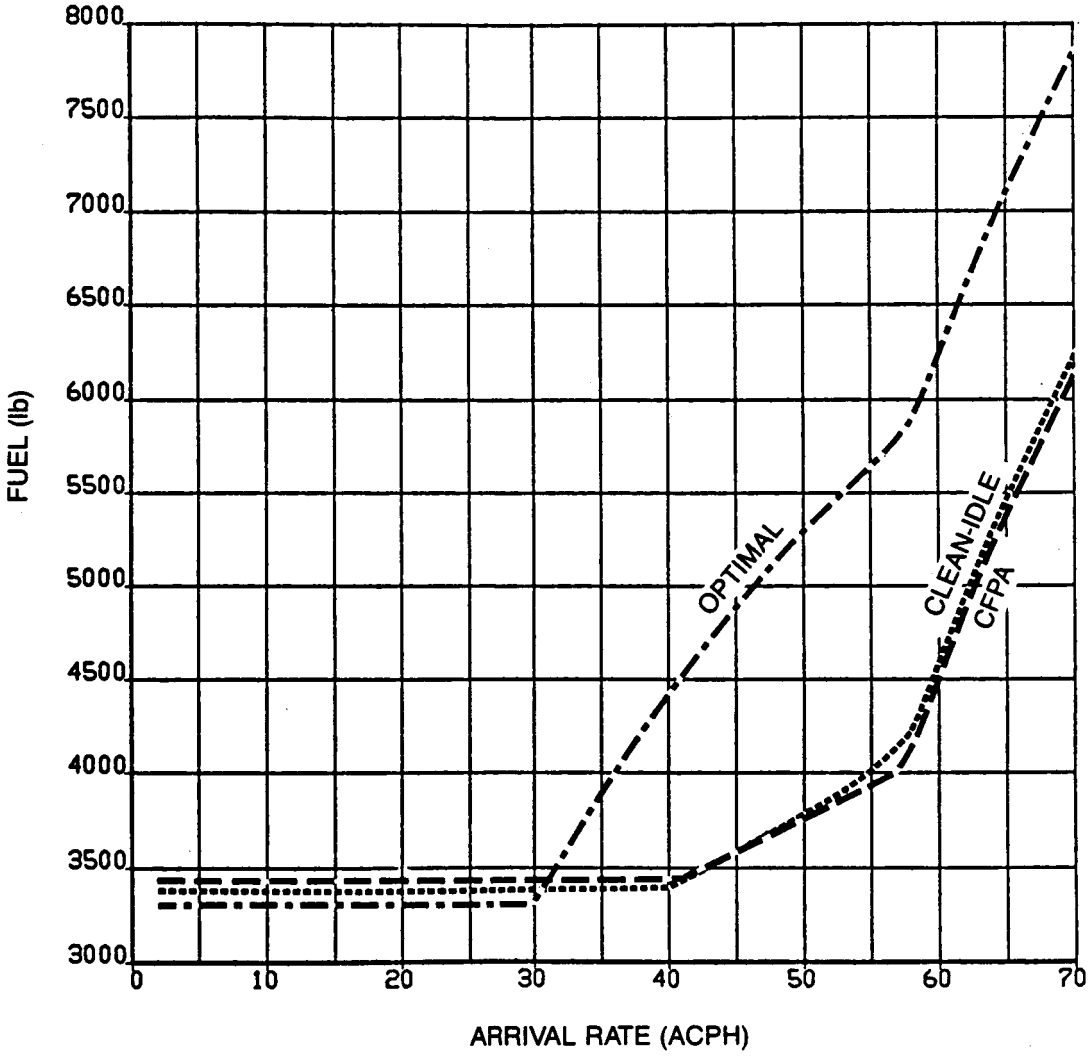

Figure B.2. Fuel Usage (Per Airplane), JFK International Airport Distribution (Average of 1000 Runs; 120 Airplane Pairs)

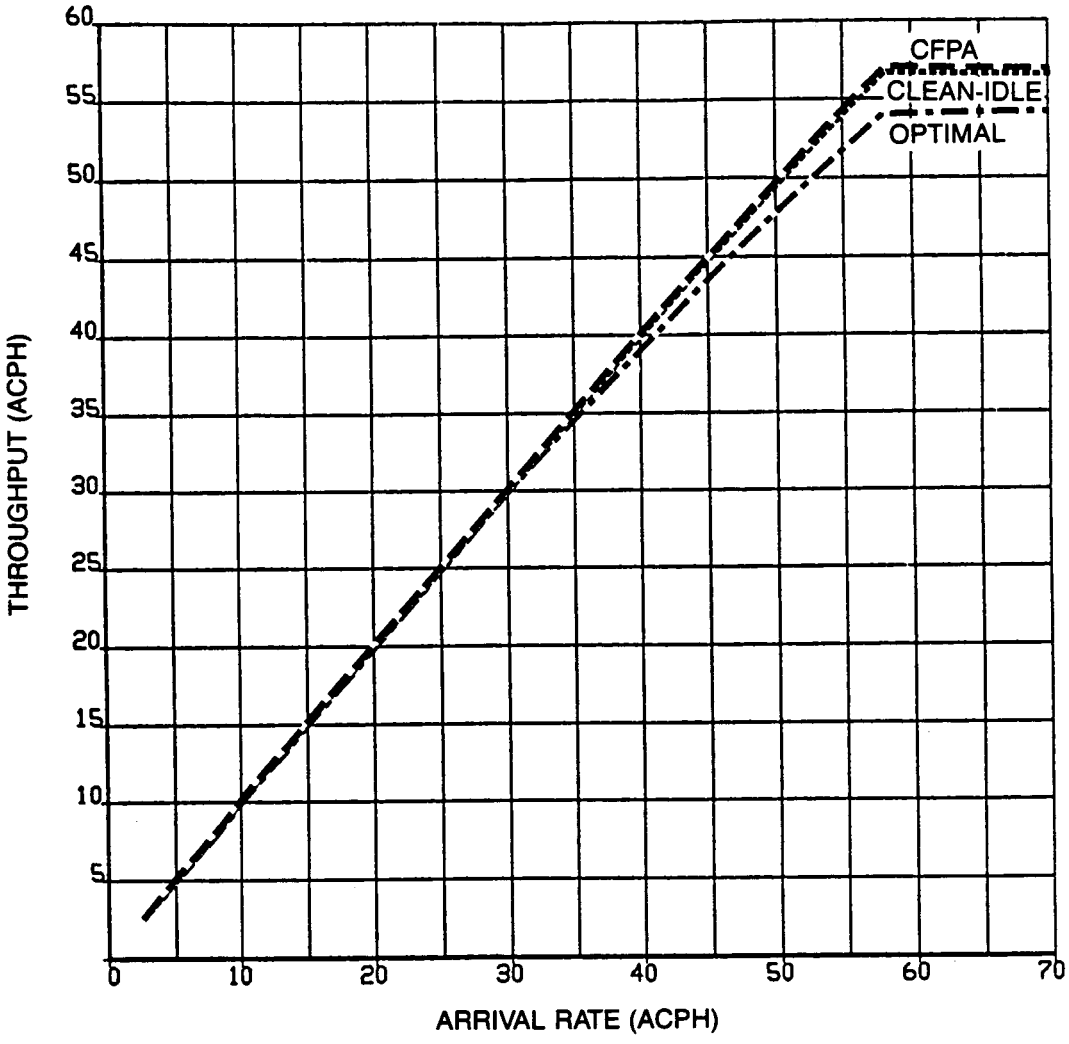

Figure B.3. Meter Fix Throughput, Typical ERM Airport Distribution (Average of 1000 Runs; 120 Airplane Pairs)

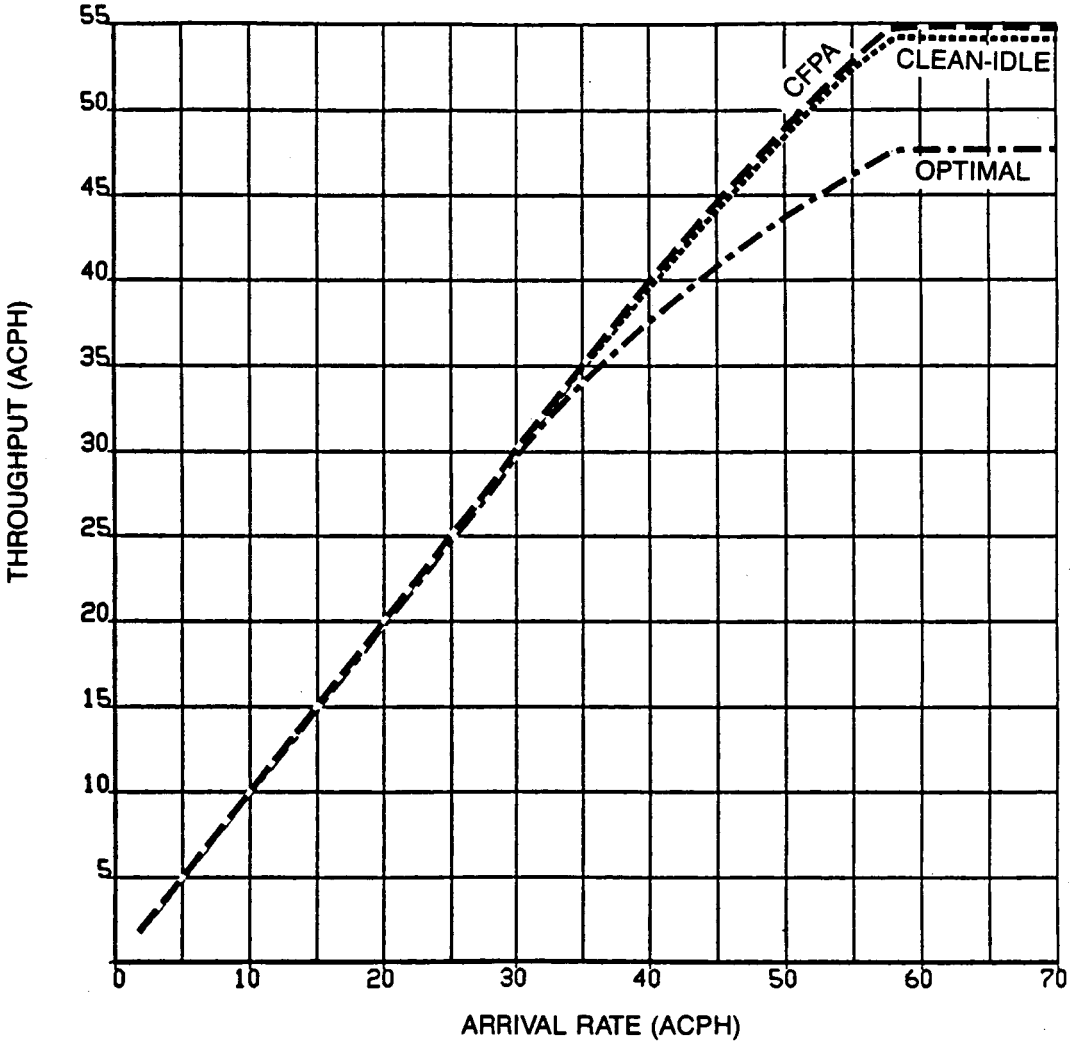

Figure B.4. Meter Fix Throughput, JFK International Airport Distribution (Average of 1000 Runs; 120 Airplane Pairs)

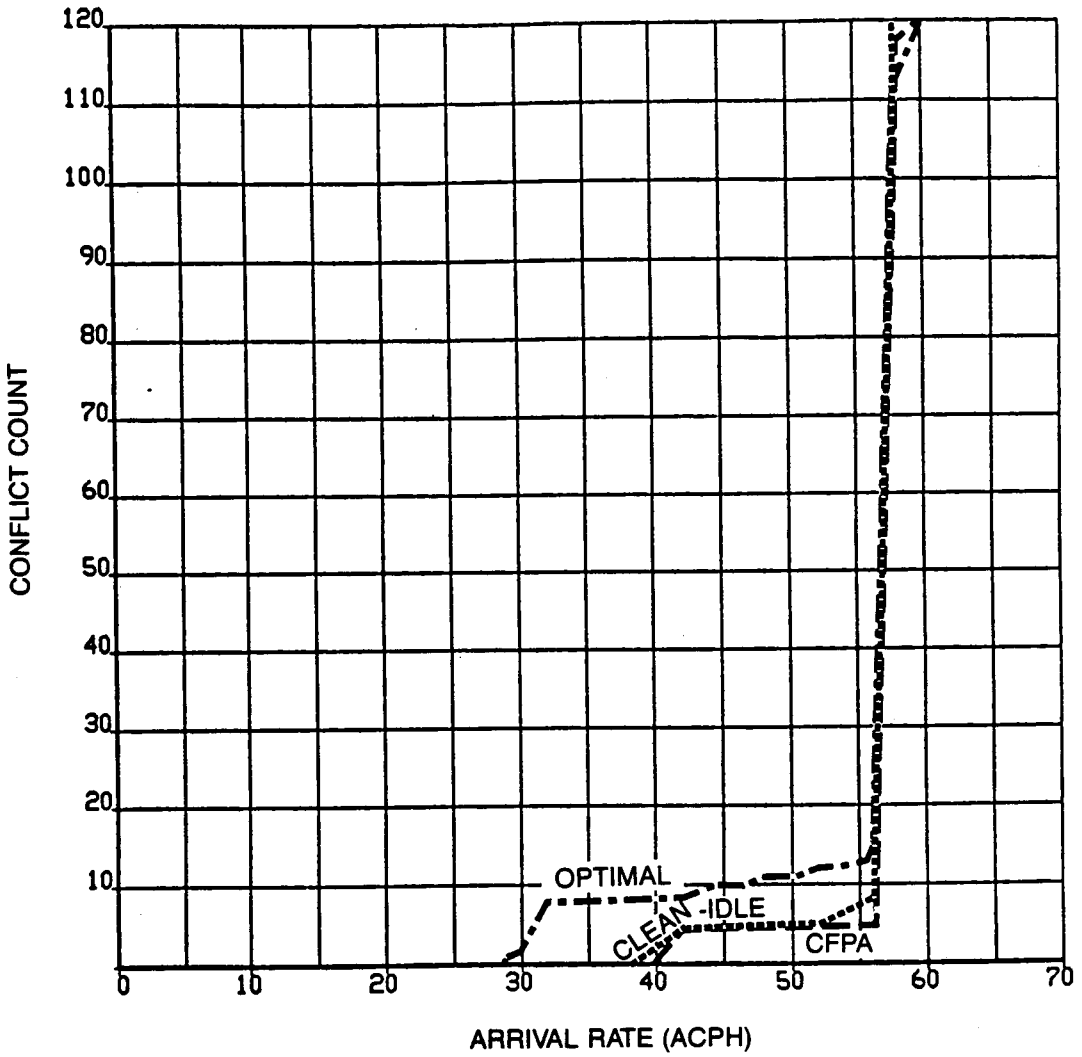

Figure B.5. Conflict Workload, Typical ERM Airport Distribution (Average of 1000 Runs; 120 Airplane Pairs)

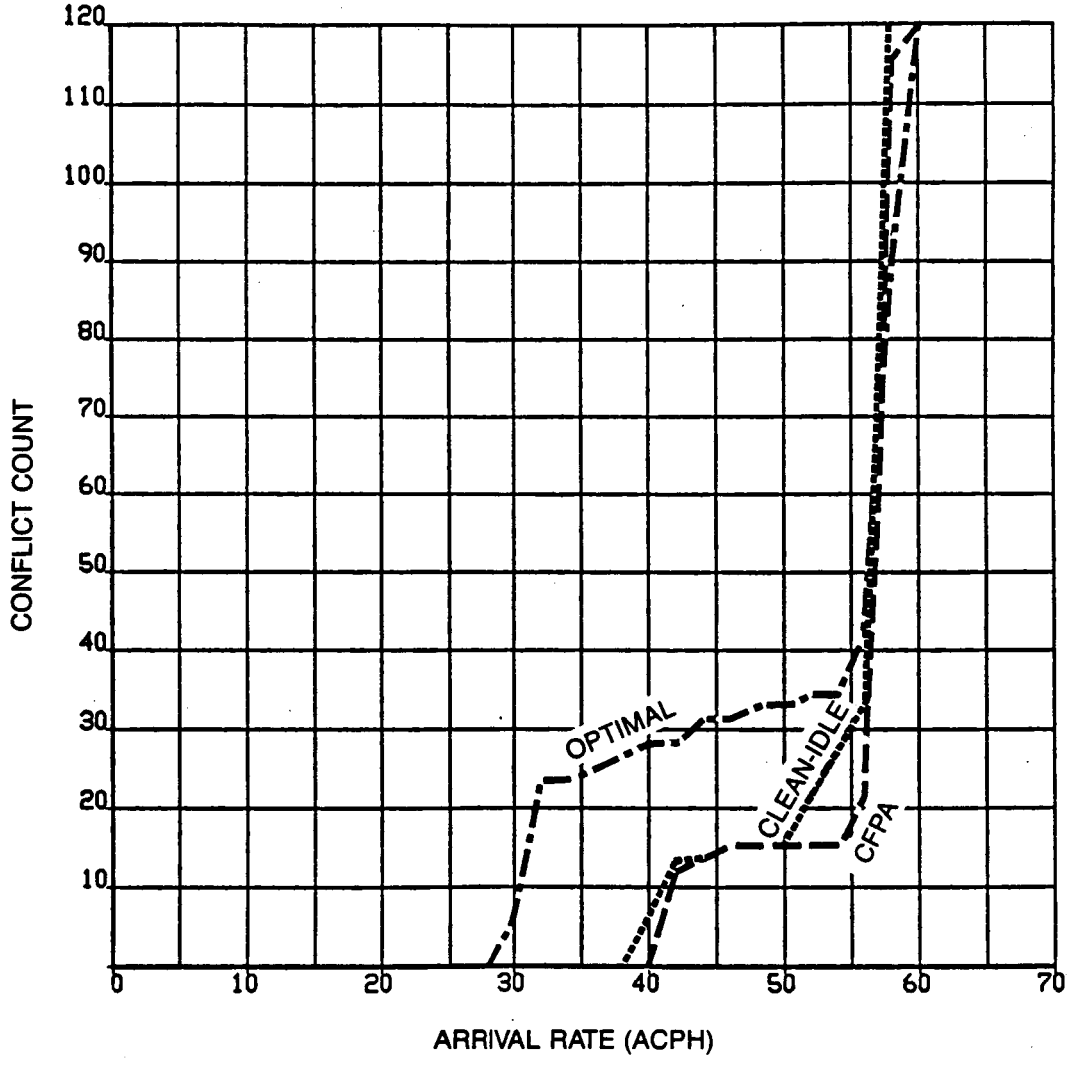

Figure B.6. Conflict Workload, JFK International Airport Distribution (Average of 1000 Runs; 120 Airplane Pairs)

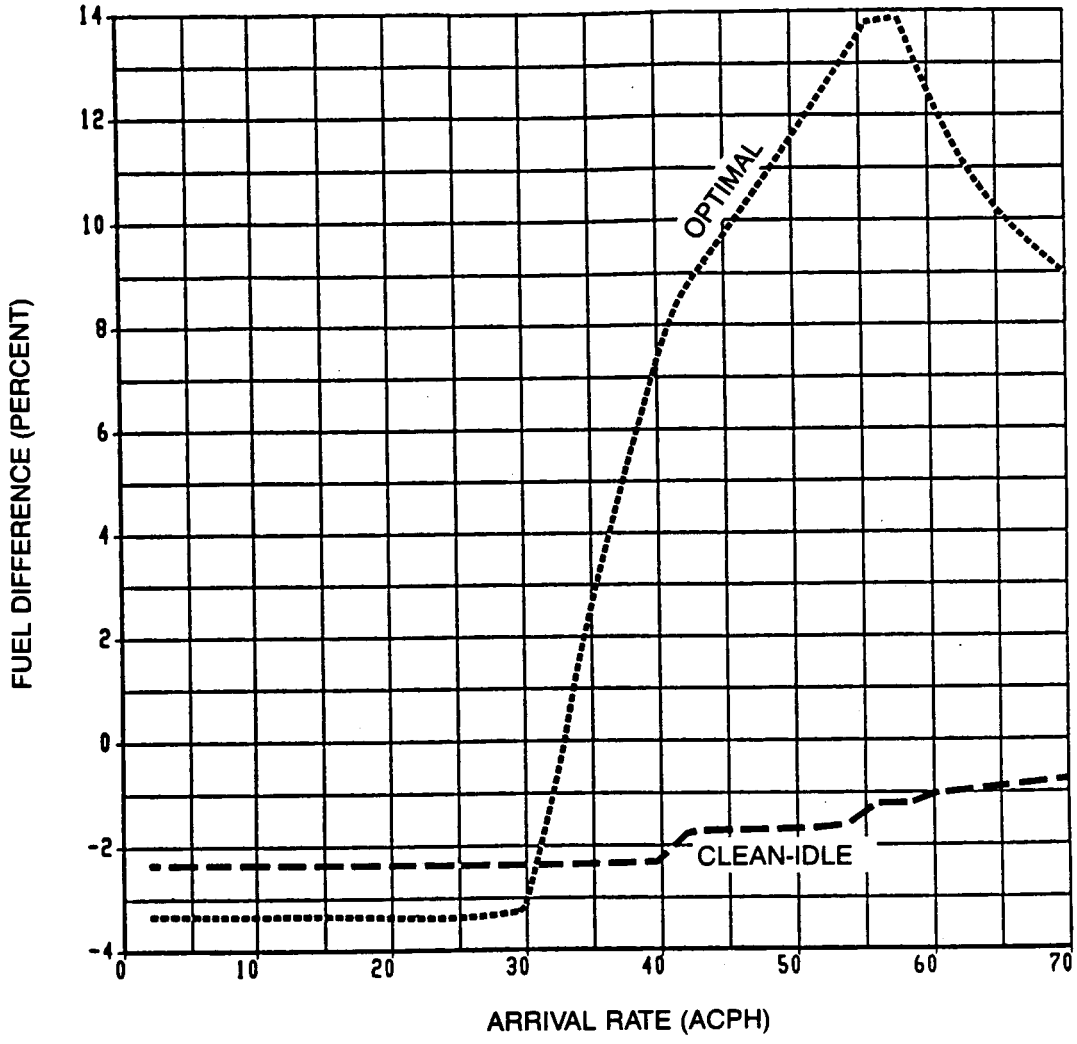

Figure B.7. Fuel Usage Penalty Relative to CFPA, Typical ERM Airport Distribution (Average of 1000 Runs; 120 Airplane Pairs)

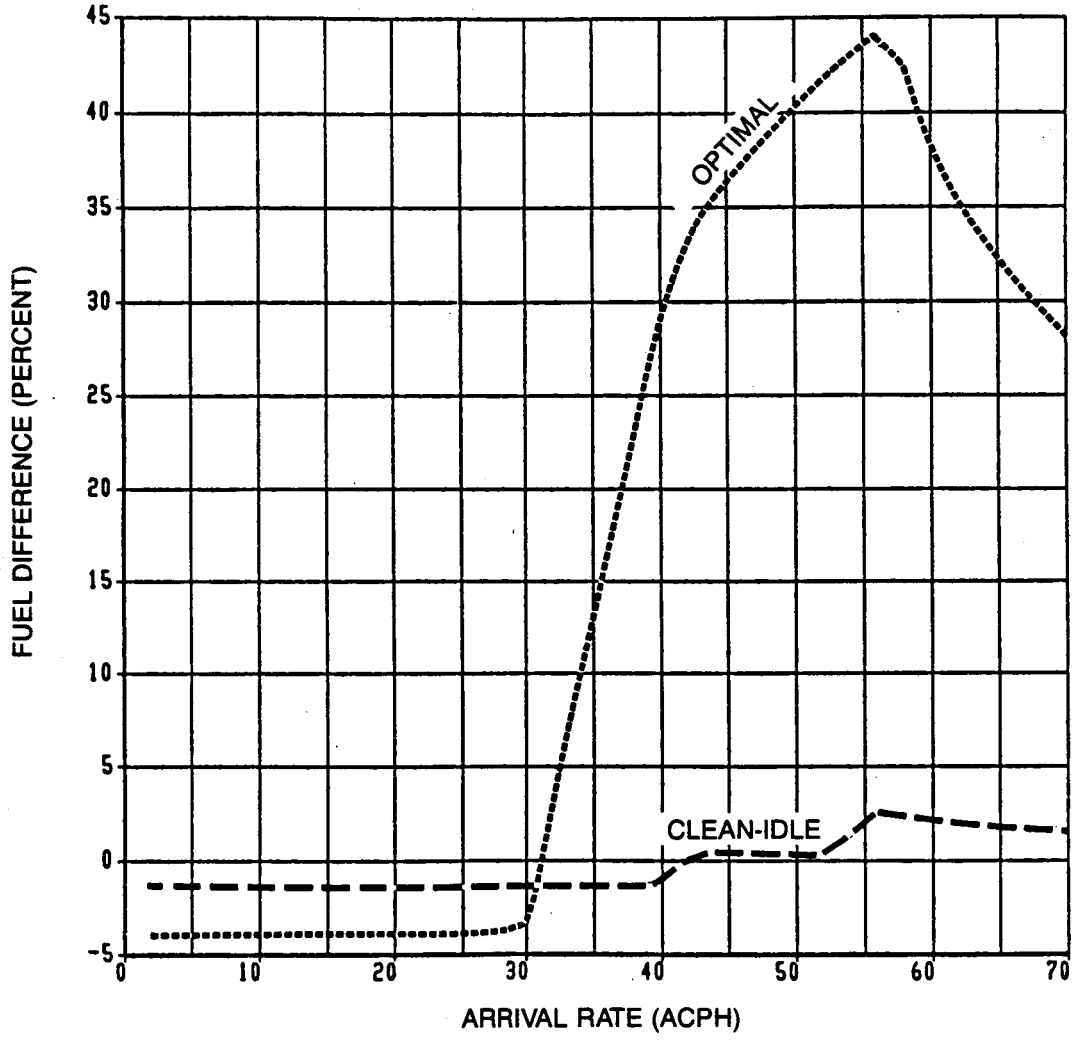

Figure B.8. Fuel Usage Penalty Relative to CFPA, JFK International Airport Distribution (Average of 1000 Runs; 120 Airplane Pairs)

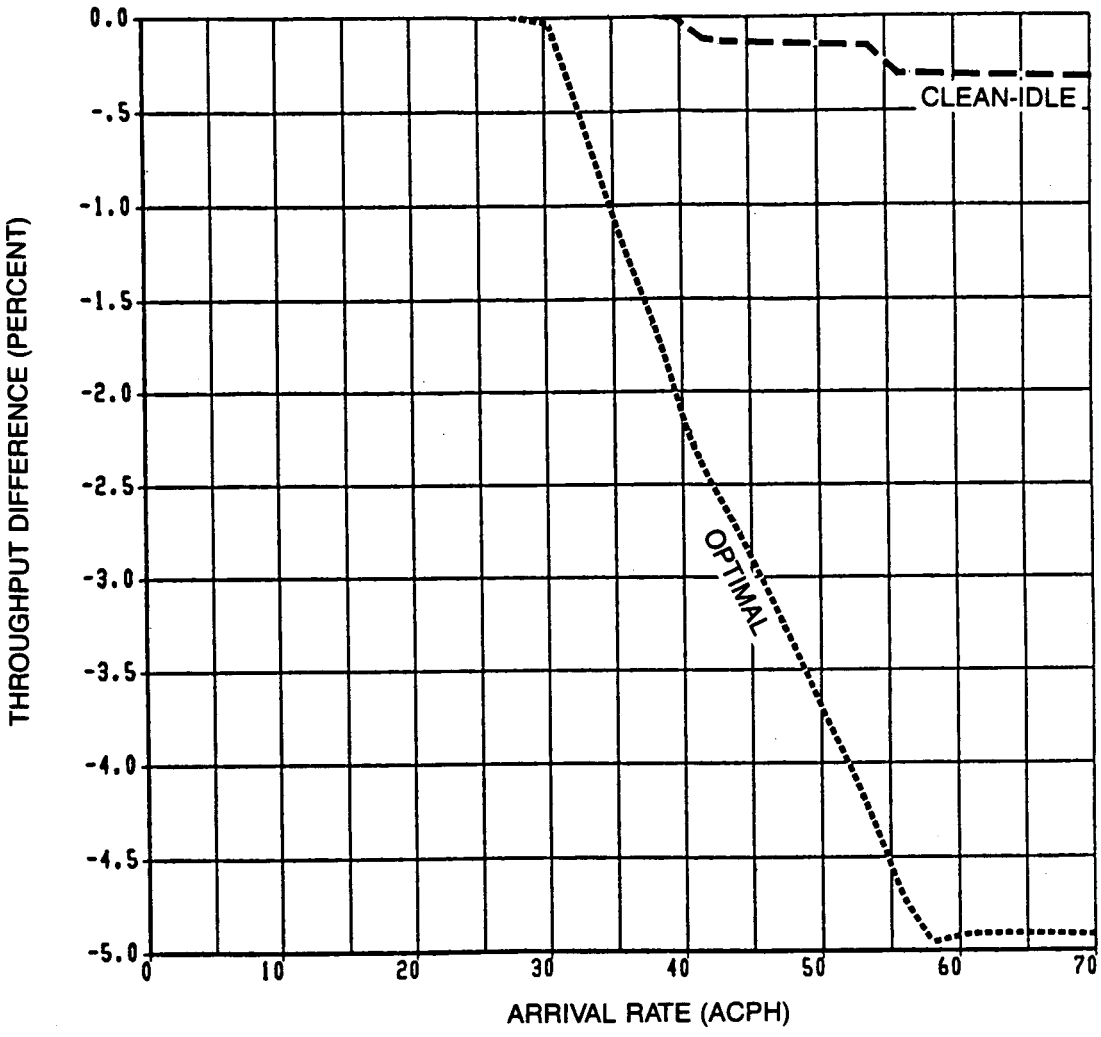

Figure B.9. Throughput Gain Relative to CFPA, Typical ERM Airport Distribution (Average of 1000 Runs; 120 Airplane Pairs)

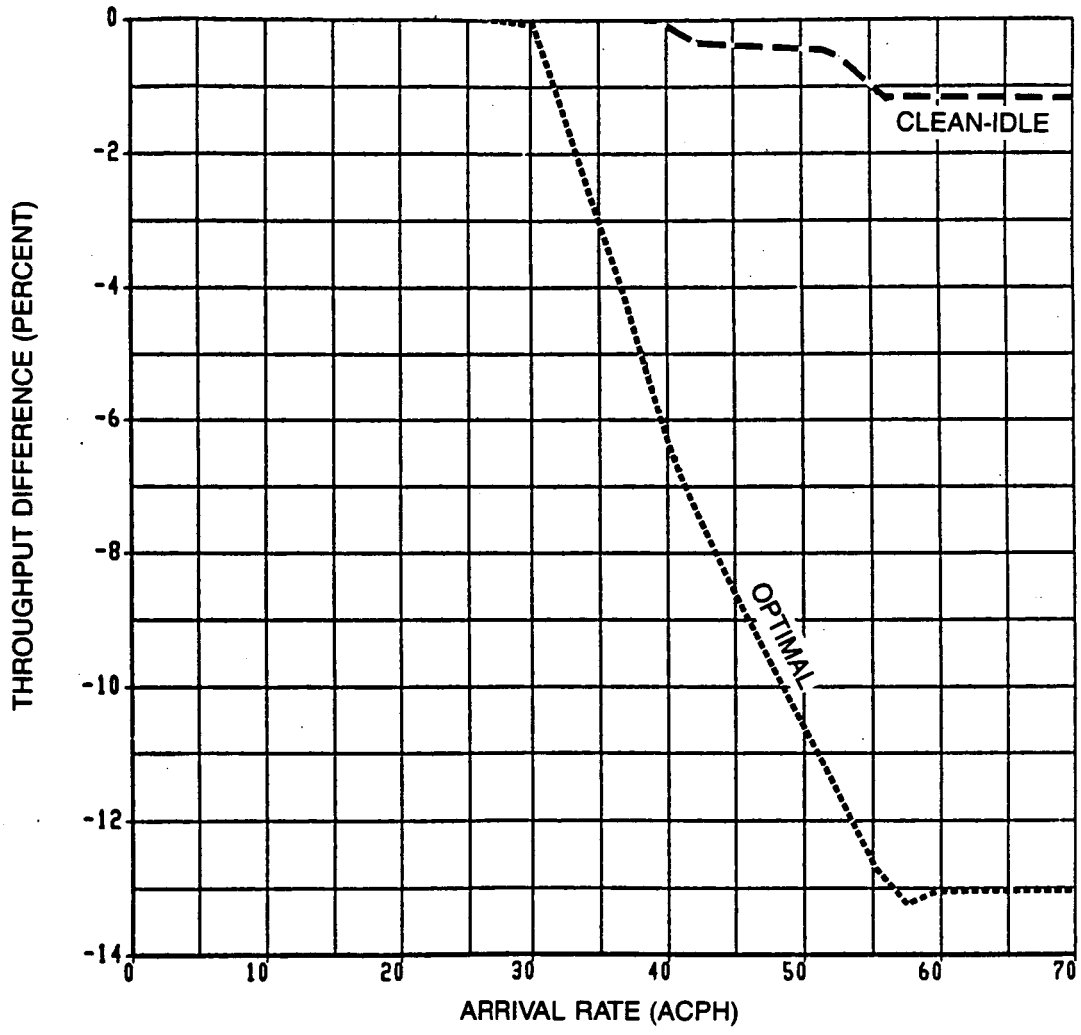

Figure B.10. Throughput Gain Relative to CFPA, JFK International Airport Distribution (Average of 1000 Runs; 120 Airplane Pairs)

1. Report No.	2. Government Accession No.	3. Recipient's Catalog No.
NASA CR-178093		

4. Title and Subtitle	5. Report Date
An Evaluation of Descent Strategies for TNAV-Equipped Aircraft in an Advanced Metering Environment	October 1986
	6. Performing Organization Code
7. Author(s)	8. Performing Organization Report No.
K. H. Izumi, R. W. Schwab, J. L. Groce, M. A. Coote	D6-53153
9. Performing Organization Name and Address	10. Work Unit No.
Boeing Commercial Airplane Company P.O. Box 3707 Seattle, WA 98124	11. Contract or Grant No. NAS1-17635
	13. Type of Report and Period Covered Contractor Report
12. Sponsoring Agency Name and Address National Aeronautics and Space Administration Washington, DC 20546	14. Sponsoring Agency Code

15. Supplementary Notes
Langley Technical Monitor: C. R. Spitzer
Final Report

16. Abstract

This study investigated the effects on system throughput and fleet fuel usage of arrival aircraft utilizing three 4D RNAV descent strategies (cost optimal, clean-idle Mach/CAS and constant descent angle Mach/CAS), both individually and in combination, in an advanced air traffic control metering environment. Results are presented for all mixtures of arrival traffic consisting of three Boeing commercial jet types and for all combinations of the three descent strategies for a typical en route metering airport arrival distribution.

17. Key Words (Suggested by Author(s))	18. Distribution Statement
Throughput, Fuel Usage, Time Navigation, 4D RNAV, Air Traffic Control, Descent Strategies	Unclassified—Unlimited

19. Security Classif. (of this report)	20. Security Classif. (of this page)	21. No. of Pages	22. Price
Unclassified	Unclassified	73	

FORM 0005 For sale by the National Technical Information Service, Springfield, Virginia 22161